

Color-octet mechanism in

$$\gamma + p \rightarrow J/\psi + X$$

Pyungwon Ko^{1,*}

¹*Department of Physics, Hong-Ik University, Seoul 121-791, Korea*

Jungil Lee^{2,†} and H.S. Song^{2,‡}

²*Center for Theoretical Physics and Department of Physics
Seoul National University, Seoul 151-742, Korea*

Abstract

Photoproduction of J/ψ is considered including the color-octet contributions from the various partial wave states, $^{2S+1}L_J = ^1S_0, ^3S_1$ and 3P_J . The production cross section depends on three new nonperturbative parameters defined in NRQCD, called the color-octet matrix elements. Using the color-octet matrix elements determined by fitting the J/ψ production at the Tevatron, we find that the color-octet ($c\bar{c}$)₈(1S_0 and 3P_J) contributions to the J/ψ photoproductions at the fixed target experiments and HERA are too large compared to the data on $\sigma(\gamma + p \rightarrow J/\psi + X)$ in the forward direction, the z distribution of J/ψ . The P_T^2 distribution of J/ψ and the total inelastic J/ψ production rate as a function of $\sqrt{s_{\gamma p}}$ are predicted including color-octet contributions. We also briefly digress on the $B \rightarrow J/\psi + X$ and observe the similar situation. This may be an indication that the color-octet matrix elements determined from the J/ψ production at the Tevatron, especially $\langle 0 | \mathcal{O}_8^\psi(^1S_0) | 0 \rangle$ and $\langle 0 | \mathcal{O}_8^\psi(^3P_J) | 0 \rangle$, might have been overestimated by an order of magnitude.

12.38.Bx, 12.39.Jh, 14.40.Lb

Typeset using REVTeX

*pko@phyb.snu.ac.kr

†jungil@phyb.snu.ac.kr

‡hssong@physs.snu.ac.kr

I. INTRODUCTION

In the conventional approach, the inelastic (inclusive) J/ψ photoproduction has been studied in the framework of perturbative QCD (PQCD) and the color singlet model [1]. In this model, one considers $\gamma + g \rightarrow J/\psi + g$ which can produce high p_T J/ψ 's at the ep or γp collision. However, the same approach, when applied to the J/ψ or ψ' production at the Tevatron, severely underestimates the productions rate [2]. In order to reconcile the data and PQCD predictions, a new mechanism for heavy quarkonium productions has been suggested [3], the color-octet gluon fragmentation into J/ψ . Also, the color-octet mechanism in heavy quarkonium productions at hadron colliders through the color-octet $(c\bar{c})_8$ pair in various partial wave states $^{2S+1}L_J$ has been considered beyond the color-octet gluon fragmentation approach [4], [5]. The main motivation is that inclusive Υ productions at the Tevatron also show the excess of the data over theoretical estimates of the productions based on PQCD and the color singlet model [6]. Here, the p_T of the Υ is not that high so that the gluon fragmentation picture may not be a good approximation any more. In Refs. [4] and [5], a large class of color-octet diagrams has been considered which can contribute to the J/ψ production at hadron colliders. At the partonic level, there appear new $2 \rightarrow 1$ subprocesses :

$$q\bar{q} \rightarrow (c\bar{c})(^3S_1^{(8)}), \quad (1.1)$$

$$gg \rightarrow (c\bar{c})(^1S_0^{(8)} \text{ or } ^3P_J^{(8)}), \quad (1.2)$$

at the short distance scale, and the subsequent evolution of the $(c\bar{c})_8(^{2S+1}L_J)$ object into a physical J/ψ by absorbing/emitting soft gluons at the long distance scale. The short distance process can be calculated using PQCD in powers of α_s , whereas the long distance part is treated as a new parameter $\langle 0|O_8^\psi(^{2S+1}L_J)|0\rangle$ which characterizes the probability that the color-octet $(c\bar{c})(^{2S+1}L_J)$ state evolves into a physical J/ψ . By fitting the J/ψ production at the Tevatron using the usual color-singlet production and the cascades from $\chi_c(1P)$ and the color-octet contribution, the authors of Ref. [5] determined

$$\langle 0|O_8^\psi(^3S_1)|0\rangle = (6.6 \pm 2.1) \times 10^{-3} \text{ GeV}^3, \quad (1.3)$$

$$\frac{\langle 0|O_8^\psi(^3P_0)|0\rangle}{M_c^2} + \frac{\langle 0|O_8^\psi(^1S_0)|0\rangle}{3} = (2.2 \pm 0.5) \times 10^{-2} \text{ GeV}^3 \quad (1.4)$$

for $M_c = 1.48$ GeV. Although the numerical values of two matrix elements $\langle 0|O_8^\psi(^3P_0)|0\rangle$ and $\langle 0|O_8^\psi(^1S_0)|0\rangle$ are not separately known in Eq. (1.4), one can still extract some useful information from it. Since both of the color octet matrix elements in Eq. (1.4) are positive definite, one has

$$0 < \langle 0|O_8^\psi(^1S_0)|0\rangle < (6.6 \pm 1.5) \times 10^{-2} \text{ GeV}^3, \quad (1.5)$$

$$0 < \frac{\langle 0|O_8^\psi(^3P_0)|0\rangle}{M_c^2} < (2.2 \pm 0.5) \times 10^{-2} \text{ GeV}^3. \quad (1.6)$$

These inequalities can provide us with some predictions on various quantities related with inclusive J/ψ productions in other high energy processes, which enables us to test the idea of color-octet mechanism.

Since the color-octet mechanism in heavy quarkonium production is a new idea proposed in order to resolve the ψ' anomaly at the Tevatron, it is important to test this idea in other high energy processes with inclusive heavy quarkonium productions. Up to now, the following processes have been considered : J/ψ production at the Tevatron and fixed target experiments [4] [5] [7], spin alignment of the color-octet produced J/ψ [8], the polar angle distribution of the J/ψ in the e^+e^- annihilations into $J/\psi + X$ [9], inclusive J/ψ production in B meson decays [10] and the Z^0 decays at LEP [11]. These processes also depend on the aforementioned three color-octet matrix elements in different combinations from (1.4). Thus, one can check if the color-octet mechanism provides reasonable agreements between PQCD and the experimental data on inclusive J/ψ production rates from these processes.

In the above list of various inclusive J/ψ productions at high energies, the J/ψ photoproduction is missing, however. It is the purpose of this work to study the color-octet mechanism in the J/ψ photoproduction ¹.

In Sec. II, we demonstrate how to get the inclusive production rate of a heavy quarkonium in the NRQCD formalism of Bodwin, Braaten and Lepage [14]. Then, we review briefly the γg fusion into $J/\psi + g$ in the color-singlet model in Sec. III A. Then in Sec. III B, we consider the color-octet subprocesses

$$\gamma + g \rightarrow (c\bar{c})(^1S_0^{(8)} \text{ or } ^3P_{J=0,2}^{(8)}), \quad (1.7)$$

which have not been included in previous studies. The size of these color-octet contributions to the J/ψ photoproductions are suppressed by v^4 relative to the color-singlet contributions, but of lower order in α_s . This subprocess contributes to the J/ψ photoproduction in the forward scattering (the elastic peak) with $z \approx 1$ and $P_T^2 \approx 0$. These color-octet $2 \rightarrow 1$ subprocesses can also contribute to the $2 \rightarrow 2$ subprocesses through

$$\gamma + g \rightarrow (c\bar{c})(^1S_0^{(8)} \text{ or } ^3P_J^{(8)}) + g, \quad (1.8)$$

$$\gamma + q \rightarrow (c\bar{c})(^1S_0^{(8)} \text{ or } ^3P_J^{(8)}) + q. \quad (1.9)$$

These are also resolved photon processes at lower order [$O(\alpha\alpha_s^2)$] than the color-singlet model [$O(\alpha\alpha_s^3)$] in the perturbation expansion in α_s : although the color-octet contributions are suppressed by v^4 compared to the color-singlet resolved photon process. Thus, the color-octet 1S_0 and 3P_J states can contribute to the elastic peak of the J/ψ -photoproduction as well as contribute to the resolved photon process. It is quite important to estimate the latter and compare with the resolved photon process in the color-singlet model, since it is a common statement that J/ψ -photoproduction is a good place to measure the gluon distribution function in a proton. We find that the quark contributions are small compared to the gluon contribution even if we include (1.9). When one considers Eqs. (1.8) and (1.9), one has to consider

$$\gamma + g \rightarrow (c\bar{c})(^{2S+1}L_J^{(8)}) + g, \quad (1.10)$$

¹While we were finishing this work, we received two preprints which discussed the same topic [12] [13]. We find our results agree with theirs in the case the direct comparison is possible.

although it is expected to be suppressed relative to the usual γg fusion color-singlet diagram by v^4 . It is gauge invariant by itself, and thus can be safely neglected if we wish. We keep it however, in order to be consistent in the α_s expansion, and make it sure the v^2 scaling rule works in this case. All of these color-octet $2 \rightarrow 2$ subprocesses are discussed in Sec. III C. Numerical analyses relevant to the fixed target experiments and HERA are performed in Sec. IV A. We show that the relations (1.5) and (1.6) yields too large a cross section for the J/ψ photoproduction in the forward direction. They also leads to too rapidly growing $d\sigma/dz$ distribution for high z region compared to the experimental observations. In Sec. IV B, we briefly digress on the $B \rightarrow J/\psi + X$ using the factorization formula derived in Ref. [10], and find again that the relations (1.5) and (1.6) overestimate the branching ratio for $B \rightarrow J/\psi + X$. All of these seem to indicate that the relations (1.3) and (1.4), especially the latter, are probably overestimated by an order of magnitude. This is not surprising at all, since the analyses in Ref. [5] employed the leading order calculations for the color-singlet parton subprocess for the J/ψ hadroproduction. We summarize our results and speculate the origins of these overestimates of J/ψ photoproductions and B meson decays in Sec. V.

II. NRQCD FORMALISM FOR HEAVY QUARKONIUM PRODUCTIONS

To begin, we consider general methods to get the NRQCD cross section of the process $a + b \rightarrow Q\bar{Q}({}^{2S+1}L_J^{(1,8a)}) \rightarrow H$, where H is the final quarkonium state and $Q\bar{Q}({}^{2S+1}L_J^{(1,8a)})$ is the intermediate $Q\bar{Q}$ pair which fragments into a specific heavy quarkonium state in the long distance scale. If the on-shell scattering amplitude of the process $\mathcal{A}(a + b \rightarrow Q + \bar{Q})$ is given, we can expand the amplitude in terms of relative momentum q of the quarks inside the bound state because the quarks which make the bound state are heavy. Scattering amplitude of the process $a + b \rightarrow Q\bar{Q}({}^{2S+1}L_J^{(1,8a)})(P)$ is given by

$$\begin{aligned} \mathcal{A}(a + b \rightarrow Q\bar{Q}({}^{2S+1}L_J^{(1,8a)})(P)) &= \sum_{L_Z S_Z} \sum_{s_1 s_2} \sum_{ij} \int \frac{d^3\vec{q}}{(2\pi)^3 2q^0} \delta(q^0 - \frac{|\vec{q}|^2}{2M_Q}) Y_{LL_Z}^*(\hat{q}) \\ &\quad \times \langle s_1; s_2 | SS_Z \rangle \langle LL_Z; SS_Z | JJ_Z \rangle \langle 3i\bar{3}j | 1, 8a \rangle \\ &\quad \times \mathcal{A}(a + b \rightarrow Q^i(\frac{P}{2} + q) + \bar{Q}^j(\frac{P}{2} - q)), \end{aligned} \quad (2.1)$$

where the superscript $(1, 8a)$ represents the color-singlet or the color-octet configuration of the $Q\bar{Q}$ state. After integrating over the relative momentum q , we get

$$\mathcal{A}(a + b \rightarrow Q\bar{Q}({}^{2S+1}L_J^{(1,8a)})) = \sqrt{C_L} \mathcal{M}'_L(a + b \rightarrow Q\bar{Q}({}^{2S+1}L_J^{(1,8a)})), \quad (2.2)$$

where

$$\begin{aligned} \mathcal{M}'_L(a + b \rightarrow Q\bar{Q}({}^{2S+1}L_J^{(1,8a)})) &= \sum_{L_Z S_Z} \sum_{s_1 s_2} \sum_{ij} \langle s_1; s_2 | SS_Z \rangle \langle LL_Z; SS_Z | JJ_Z \rangle \langle 3i\bar{3}j | 1, 8a \rangle \\ &\quad \times \begin{cases} \mathcal{A}(a + b \rightarrow Q^i + \bar{Q}^j)|_{q=0} & (L = S), \\ \epsilon_{\alpha}^*(L_Z) \mathcal{A}^{\alpha}(a + b \rightarrow Q^i + \bar{Q}^j)|_{q=0} & (L = P), \\ \epsilon_{\alpha\beta}^*(L_Z) \mathcal{A}^{\alpha\beta}(a + b \rightarrow Q^i + \bar{Q}^j)|_{q=0} & (L = D), \end{cases} \end{aligned} \quad (2.3)$$

$$C_L = \frac{M_Q^3}{2q^0(2\pi)^5} \times |\vec{q}|^{2L} \quad \text{and} \quad C_L^{rel} = \frac{M_Q^3}{2q^0(2\pi)^5} \times |\vec{q}|^{2L+2}. \quad (2.4)$$

Here, C_L^{rel} is the factor for the relativistic correction of the L state. From now on, amplitudes with Lorentz indices mean

$$A^\alpha(P, q) = \frac{\partial}{\partial q^\alpha} A(P, q) \quad \text{and} \quad A^{\alpha\beta}(P, q) = \frac{\partial^2}{\partial q^\alpha \partial q^\beta} A(P, q). \quad (2.5)$$

The color SU(3) coefficients are given by

$$\langle 3i; \bar{3}j | 1 \rangle = \delta_{ij} / \sqrt{N_c} \quad \text{and} \quad \langle 3i; \bar{3}j | 8a \rangle = \sqrt{2} T_{ij}^a. \quad (2.6)$$

For the case of color singlet state, we can relate the coefficients C_L to the radial wavefunction of the bound state as

$$C_S = \frac{1}{4\pi} |R_S(0)|^2, \quad C_P = \frac{3}{4\pi} |R'_P(0)|^2 \quad \text{and} \quad C_D = \frac{15}{8\pi} |R''_D(0)|^2. \quad (2.7)$$

Some identities of color matrix trace are useful in squaring the matrix elements.

$$\begin{aligned} \text{Tr}(1) &= +N_c, & \text{Tr}(T^a T^b T^c T^c T^b T^a) &= +\frac{(N_c^2 - 1)^3}{8N_c^2}, \\ \text{Tr}(T^a T^a) &= +\frac{N_c^2 - 1}{2}, & \text{Tr}(T^a T^b T^c T^b T^c T^a) &= -\frac{(N_c^2 - 1)^2}{8N_c^2}, \\ \text{Tr}(T^a T^b T^b T^a) &= +\frac{N_c^2 - 1}{4N_c}, & \text{Tr}(T^a T^b T^c T^a T^b T^c) &= +\frac{(N_c^4 - 1)}{8N_c^2}, \\ \text{Tr}(T^a T^b T^a T^b) &= -\frac{N_c^2 - 1}{4N_c}, & \text{Tr}(T^a T^b T^c) \text{Tr}(T^a T^b T^c) &= -\frac{(N_c^2 - 1)}{4N_c}, \\ \text{Tr}(T^a T^b) \text{Tr}(T^a T^b) &= +\frac{N_c^2 - 1}{4}, & \text{Tr}(T^a T^b T^c) \text{Tr}(T^a T^c T^b) &= -\frac{(N_c^2 - 1)(N_c^2 - 2)}{4N_c}. \end{aligned} \quad (2.8)$$

At this stage we can derive the explicit form of the matrix element \mathcal{M}'_L . In general, the on-shell amplitude can be expressed as

$$\langle 3i\bar{3}j | 1, 8a \rangle \mathcal{A}(a + b \rightarrow Q^i(\frac{P}{2} + q) + \bar{Q}^j(\frac{P}{2} - q)) = \bar{u}(\frac{P}{2} + q; s_1) \mathcal{O}(P, q) v(\frac{P}{2} - q; s_2), \quad (2.9)$$

where \mathcal{O} is the matrix relevant to the on shell amplitude. If we introduce the spin projection operator $P_{SS_z}(P, q)$ as

$$P_{SS_z}(P, q)_{ij} \equiv \sum_{s_1 s_2} \langle s_1; s_2 | SS_z \rangle v_i(\frac{P}{2} - q; s_2) \bar{u}_j(\frac{P}{2} + q; s_1), \quad (2.10)$$

we can simplify the form of the matrix element \mathcal{M}'_L as

$$\mathcal{M}'_S = \text{Tr} [\mathcal{O}(P, 0) P_{SS_z}(P, 0)], \quad (2.11)$$

$$\mathcal{M}'_P = \sum_{L_z S_z} \epsilon_\alpha^*(L_z) \langle LL_z; SS_z | JJ_z \rangle \text{Tr} [\mathcal{O}^\alpha P_{SS_z} + \mathcal{O} P_{SS_z}^\alpha]_{q=0}, \quad (2.12)$$

$$\mathcal{M}'_D = \sum_{L_z S_z} \epsilon_{\alpha\beta}^*(L_z) \langle LL_z; SS_z | JJ_z \rangle \text{Tr} [\mathcal{O}^{\alpha\beta} P_{SS_z} + \mathcal{O}^\alpha P_{SS_z}^\beta + \mathcal{O}^\beta P_{SS_z}^\alpha + \mathcal{O} P_{SS_z}^{\alpha\beta}]_{q=0}. \quad (2.13)$$

Note that \mathcal{O} includes the color coefficient $\langle 3i\bar{3}j | 1, 8a \rangle$ and P_{SS_z} possesses the spin coefficient $\langle s_1; s_2 | SS_z \rangle$. Expanding $P_{SS_z}(P, q)$ to the second order of the relative momentum q , we get

$$P_{00}(P, 0) = \frac{1}{2\sqrt{2}}\gamma_5(\not{P} + 2M_Q), \quad (2.14)$$

$$P_{00}^\alpha(P, 0) = \frac{1}{2\sqrt{2}M_Q}\gamma^\alpha\gamma_5\not{P}, \quad (2.15)$$

$$P_{00}^{\alpha\beta}(P, 0) = -\frac{1}{2\sqrt{2}M_Q}g^{\alpha\beta}\gamma_5, \quad (2.16)$$

$$P_{1S_z}(P, 0) = \frac{1}{2\sqrt{2}}\not{\epsilon}^*(S_z)(\not{P} + 2M_Q), \quad (2.17)$$

$$P_{1S_z}^\alpha(P, 0) = \frac{1}{4\sqrt{2}M_Q}[\not{\epsilon}^*(S_z)(\not{P} + 2M_Q)\gamma^\alpha + \gamma^\alpha\not{\epsilon}^*(S_z)(\not{P} + 2M_Q)], \quad (2.18)$$

$$P_{1S_z}^{\alpha\beta}(P, 0) = -\frac{1}{2\sqrt{2}M_Q}\left[g^{\alpha\beta}\not{\epsilon}^*(S_z) - \frac{1}{4M_Q}(\not{P} + 2M_Q)(\epsilon^{*\alpha}(S_z)\gamma^\beta + \epsilon^{*\beta}(S_z)\gamma^\alpha)\right]. \quad (2.19)$$

When $L = P$, we need further relations to get the correct polarization state of the intermediate state,

$$\begin{aligned} \sum_{L_z S_z} \epsilon^{*\alpha(L_z)} \epsilon^{*\beta}(S_z) \langle 1L_z; 1S_z | J = 0 \ J_z = 0 \rangle &= \frac{1}{\sqrt{3}} \left(-g^{\alpha\beta} + \frac{P^\alpha P^\beta}{M^2} \right), \\ \sum_{L_z S_z} \epsilon^{*\alpha(L_z)} \epsilon^{*\beta}(S_z) \langle 1L_z; 1S_z | J = 1 \ J_z \rangle &= -\frac{i}{\sqrt{2}M} \epsilon^{\alpha\beta\lambda\kappa} P_\kappa \epsilon_\lambda^*(J_z), \\ \sum_{L_z S_z} \epsilon^{*\alpha(L_z)} \epsilon^{*\beta}(S_z) \langle 1L_z; 1S_z | J = 2 \ J_z \rangle &= \epsilon^{*\alpha\beta}(J_z), \end{aligned} \quad (2.20)$$

where the polarization vector and symmetric polarization tensor have the properties

$$P_\alpha \epsilon^\alpha(J_z) = 0, \quad P_\alpha \epsilon^{\alpha\beta}(J_z) = 0, \quad \epsilon_\alpha^\alpha(J_z) = 0, \quad \epsilon^{\alpha\beta}(J_z) = \epsilon^{\beta\alpha}(J_z). \quad (2.21)$$

Once the cross section of the on-shell parton level process is calculated, one can expand it in factorized forms following BBL [14] as

$$\hat{\sigma}(a + b \rightarrow (Q\bar{Q})_n) = \frac{F_n}{M_Q^{d_n-5}} \times \frac{\langle 0 | \mathcal{O}_n^{Q\bar{Q}} | 0 \rangle}{2J+1}, \quad (2.22)$$

$$\hat{\sigma}(a + b \rightarrow (Q\bar{Q})_n \rightarrow H + X) = \frac{F_n}{M_Q^{d_n-4}} \times \frac{\langle 0 | \mathcal{O}_n^H | 0 \rangle}{2J+1}. \quad (2.23)$$

We use $\hat{\sigma}$ instead of σ , as a subprocess cross section, since we will consider γp collision where the particle b is treated as a parton inside a proton. The index n denotes the intermediate $Q\bar{Q}$ state $^{2S+1}L_J^{(1,8)}$, which may differ from that of H . The factor multiplied to the H production cross section differs from that of $Q\bar{Q}$ state by unity in mass dimension. This makes the long range factor coincide with the conventionally normalized wave function of the bound state for the color singlet case. We extracted the factor $1/(2J+1)$ in advance to avoid the unnecessary factor after imposing the heavy quark spin symmetry property as

$$\frac{\langle 0 | \mathcal{O}^\psi(^3S_1^{(1,8)}) | 0 \rangle}{3} \rightarrow \langle 0 | \mathcal{O}^\psi(^1S_0^{(1,8)}) | 0 \rangle, \quad (2.24)$$

$$\frac{\langle 0 | \mathcal{O}^\psi(^3P_J^{(1,8)}) | 0 \rangle}{2J+1} \rightarrow \langle 0 | \mathcal{O}^\psi(^3P_0^{(1,8)}) | 0 \rangle. \quad (2.25)$$

The 4-fermion operator \mathcal{O}_n with the dimension d_n are defined as

$$\begin{aligned}
d_n = 6 & & d_n = 8 \\
\mathcal{O}_1(^1S_0) &= \psi^\dagger \chi \chi^\dagger \psi, & \mathcal{O}_1(^1P_1) &= \psi^\dagger (-\frac{i}{2} \overleftrightarrow{D}) \chi \cdot \chi^\dagger (-\frac{i}{2} \overleftrightarrow{D}) \psi, \\
\mathcal{O}_8(^1S_0) &= \psi^\dagger T^a \chi \chi^\dagger T^a \psi, & \mathcal{O}_1(^3P_0) &= \frac{1}{3} \psi^\dagger (-\frac{i}{2} \overleftrightarrow{D} \cdot \vec{\sigma}) \chi \chi^\dagger (-\frac{i}{2} \overleftrightarrow{D} \cdot \vec{\sigma}) \psi, \\
\mathcal{O}_1(^3S_1) &= \psi^\dagger \vec{\sigma} \chi \cdot \chi^\dagger \vec{\sigma} \psi, & \mathcal{O}_1(^3P_1) &= \frac{1}{2} \psi^\dagger (-\frac{i}{2} \overleftrightarrow{D} \times \vec{\sigma}) \chi \cdot \chi^\dagger (-\frac{i}{2} \overleftrightarrow{D} \times \vec{\sigma}) \psi, \\
\mathcal{O}_8(^3S_1) &= \psi^\dagger \vec{\sigma} T^a \chi \cdot \chi^\dagger \vec{\sigma} T^a \psi, & \mathcal{O}_1(^3P_2) &= \psi^\dagger (-\frac{i}{2} \overleftrightarrow{D}^{(i\sigma^j)}) \chi \cdot \chi^\dagger (-\frac{i}{2} \overleftrightarrow{D}^{(i\sigma^j)}) \psi.
\end{aligned} \tag{2.26}$$

and dimension-8 operators related to the relativistic correction are

$$\begin{aligned}
\mathcal{P}_1(^1S_0) &= \frac{1}{2} \left[\psi^\dagger \chi \chi^\dagger (-\frac{i}{2} \overleftrightarrow{D})^2 \psi + \text{h.c.} \right], \\
\mathcal{P}_1(^3S_1) &= \frac{1}{2} \left[\psi^\dagger \vec{\sigma} \chi \cdot \chi^\dagger \vec{\sigma} (-\frac{i}{2} \overleftrightarrow{D})^2 \psi + \text{h.c.} \right], \\
\mathcal{P}_1(^3S_1, ^3D_1) &= \frac{1}{2} \left[\psi^\dagger \sigma^i \chi \chi^\dagger \sigma^j (-\frac{i}{2})^2 \overleftrightarrow{D}^{(i\overleftrightarrow{D}^j)} \psi + \text{h.c.} \right].
\end{aligned} \tag{2.27}$$

where

$$\chi^\dagger \overleftrightarrow{D} \psi \equiv \chi^\dagger (\overrightarrow{D} \psi) - (\overrightarrow{D} \chi)^\dagger \psi, \tag{2.28}$$

$$A^{(ij)} = \frac{1}{2} (A^{ij} + A^{ji}) - \frac{1}{3} \text{Tr}(A) \delta^{ij}, \tag{2.29}$$

and \overrightarrow{D} is the covariant derivative. There are Pauli spinor fields in the previous equations. ψ annihilates a heavy quark Q and χ creates a heavy antiquark \bar{Q} . Color and spin indices on the fields ψ, χ have been suppressed.

Vacuum expectation values of the production operators $\mathcal{O}_n^{Q\bar{Q}}$ and \mathcal{O}_n^H are

$$\langle 0 | \mathcal{O}_n^H | 0 \rangle = \langle 0 | \chi^\dagger \mathcal{K}_n \psi \left(\sum_X \sum_{m_J} |H + X\rangle \langle H + X| \right) \psi^\dagger \mathcal{K}'_n \chi | 0 \rangle, \tag{2.30}$$

$$\begin{aligned}
\langle 0 | \mathcal{O}_n^{Q\bar{Q}} | 0 \rangle &= \langle 0 | \chi^\dagger \mathcal{K}_n \psi \left(\sum_{m_J} |Q\bar{Q}(^{2S+1}L_J^{(1,8)})\rangle \langle Q\bar{Q}(^{2S+1}L_J^{(1,8)})| \right) \psi^\dagger \mathcal{K}'_n \chi | 0 \rangle \\
&= (2J + 1) \langle 0 | \chi^\dagger \mathcal{K}_n \psi | Q\bar{Q}(^{2S'+1}L_0^{(8)}) \rangle \langle Q\bar{Q}(^{2S'+1}L_0^{(1,8)}) | \psi^\dagger \mathcal{K}'_n \chi | 0 \rangle \\
&= (2J + 1) \langle 0 | \mathcal{O}^{Q\bar{Q}}(^{2S'+1}L_0^{(1,8)}) | 0 \rangle.
\end{aligned} \tag{2.31}$$

The factors \mathcal{K}_n and \mathcal{K}'_n are products of a color matrix, a spin matrix and a polynomial in the covariant derivative \overleftrightarrow{D} and other fields, which are same with those of \mathcal{O}_n . According to the heavy quark spin symmetry, $^{2S+1}L_J^{(1,8)}$ state has the same properties with another state $^{2S'+1}L_0^{(1,8)}$ (with the same L) except for the m_J multiplicity factor $2J + 1$, which appears in the last equation.

Let us explain the process to derive the short distance coefficients F_n . Regardless of the onshell scattering amplitude $a + b \rightarrow Q + \bar{Q}$, the intermediate bound state $Q\bar{Q}(^{2S+1}L^{(1,8)})$ production cross sections have common factor $\langle 0 | \mathcal{O}_n^{Q\bar{Q}} | 0 \rangle$. We can obtain the matrix elements by using the intermediate state ket

$$\begin{aligned}
|Q\bar{Q}(^{2S+1}L_J^{(1,8a)})(P)\rangle &= \sum_{L_Z S_Z} \sum_{s_1 s_2} \sum_{ij} \int \frac{d^3 \vec{q}}{(2\pi)^3 2q^0} \delta(q^0 - \frac{|\vec{q}|^2}{2M_Q}) Y_{LL_Z}^*(\hat{q}) \\
&\times \langle s_1; s_2 | SS_Z \rangle \langle LL_Z; SS_Z | JJ_Z \rangle \langle 3i\bar{3}j | 1, 8a \rangle |Q^i(\frac{P}{2} + q) \bar{Q}^j(\frac{P}{2} - q)\rangle \tag{2.32}
\end{aligned}$$

as

$$\frac{\langle 0 | \mathcal{O}_n^{Q\bar{Q}} | 0 \rangle}{2J+1} = C_L \times C_n, \quad (2.33)$$

where

$$C_n = \begin{cases} 2N_c & (\text{color singlet}) \\ N_c^2 - 1 & (\text{color octet}) \end{cases}. \quad (2.34)$$

The cross section of the process $a(p_1) + b(p_2) \rightarrow (Q\bar{Q})_n(P)$ (with n representing the partial wave and the color quantum numbers of $Q\bar{Q}$) is given by

$$\begin{aligned} & \hat{\sigma}(a(p_1) + b(p_2) \rightarrow (Q\bar{Q})_n(P)) \\ &= \frac{1}{2\hat{s}} \int \frac{d^3\vec{P}}{(2\pi)^3 2E_P} (2\pi)^4 \delta^{(4)}(P - p_1 - p_2) \overline{\sum} |\mathcal{A}(a + b \rightarrow (Q\bar{Q})_n)|^2 \\ &= \hat{\sigma}'_n \times C_L \times C_n \\ &= \hat{\sigma}'_n \times \frac{\langle 0 | \mathcal{O}_n^{Q\bar{Q}} | 0 \rangle}{2J+1}, \end{aligned} \quad (2.35)$$

where

$$\hat{\sigma}'_n = \frac{1}{C_n} \frac{\pi}{\hat{s}} \delta(\hat{s} - M_P^2) \overline{\sum} |\mathcal{M}'_L(a + b \rightarrow (Q\bar{Q})_n)|^2, \quad (2.36)$$

n represents the partial wave ($^{2S+1}L_J$) and the color quantum numbers of $Q\bar{Q}$ and \hat{s} is the invariant mass of the initial particles a and b . Then, the bound state cross section and the short distance coefficients F_n are given by

$$\hat{\sigma}(a(p_1) + b(p_2) \rightarrow (Q\bar{Q})_n \rightarrow H + X) = \frac{\hat{\sigma}'_n}{M_Q} \times \frac{\langle 0 | \mathcal{O}_n^H | 0 \rangle}{2J+1} = \frac{\hat{\sigma}'_n M_Q^{d_n-5}}{M_Q^{d_n-4}} \times \frac{\langle 0 | \mathcal{O}_n^H | 0 \rangle}{2J+1}, \quad (2.37)$$

$$F_n = \hat{\sigma}'_n \times M_Q^{d_n-5}. \quad (2.38)$$

In case of γp scattering, we should convolute the above result with the parton structure functions to get the cross section :

$$\sigma(a(p_1) + b(p_2) \rightarrow (Q\bar{Q})_n \rightarrow H + X) = \frac{1}{M_Q} \sum_b \sigma'_n(b) \times \frac{\langle 0 | \mathcal{O}_n^H | 0 \rangle}{2J+1}, \quad (2.39)$$

where

$$\begin{aligned} \sigma'_n(b) &= \int dx f_{b/p}(x) \hat{\sigma}'_n \\ &= \frac{\pi}{16C_n M_Q^4} \left[x f_{b/p}(x) \right]_{x=4M_Q^2/s} \overline{\sum} |\mathcal{M}'_L(a + b \rightarrow (Q\bar{Q})_n)|^2. \end{aligned} \quad (2.40)$$

For the case of $2 \rightarrow 2$ process, we need to modify the formulae only a little. The quarkonium H photoproduction cross section via $2 \rightarrow 2$ subprocess $a(p_1) + b(P_2)/p \rightarrow (Q\bar{Q})_n(P) + c(p_3) \rightarrow H + X$, where b is a parton of the initial proton is given by

$$\begin{aligned}
d\sigma\left(a(p_1) + b(P_2)/p \rightarrow (Q\bar{Q})_n(P) + c(p_3) \rightarrow H + X\right) \\
= \frac{1}{C_n M_Q} \cdot \frac{1}{16\pi\hat{s}^2} \overline{\sum} |\mathcal{M}'\left((p_1) + b(P_2) \rightarrow (Q\bar{Q})_n(P) + c(p_3)\right)|^2 \frac{x f_{b/p}(x)}{z(1-z)} dz dP_T^2. \quad (2.41)
\end{aligned}$$

For example, if we consider the J/ψ production via $^1S_0^{(8)}$, $^3S_1^{(8)}$, $^3P_0^{(8)}$, $^3P_1^{(8)}$ and $^3P_2^{(8)}$ intermediate states, we get

$$\begin{aligned}
\hat{\sigma}(H) &= \frac{1}{M_Q} \left(\hat{\sigma}'(^1S_0^{(8)}) \times \langle 0 | \mathcal{O}^\psi(^1S_0^{(8)}) | 0 \rangle + \hat{\sigma}'(^3S_1^{(8)}) \times \frac{\langle 0 | \mathcal{O}^\psi(^3S_1^{(8)}) | 0 \rangle}{3} \right. \\
&\quad \left. + \sum_J \hat{\sigma}'(^3P_J^{(8)}) \times \frac{\langle 0 | \mathcal{O}^\psi(^3P_J^{(8)}) | 0 \rangle}{2J+1} \right) \\
&= \frac{1}{M_Q} \left[\langle 0 | \mathcal{O}^\psi(^1S_0^{(8)}) | 0 \rangle \times \left(\hat{\sigma}'(^1S_0^{(8)}) + \hat{\sigma}'(^3S_1^{(8)}) \right) + \langle 0 | \mathcal{O}^\psi(^3P_0^{(8)}) | 0 \rangle \times \sum_J \hat{\sigma}'(^3P_J^{(8)}) \right]. \quad (2.42)
\end{aligned}$$

III. J/ψ PHOTOPRODUCTION SUBPROCESSES

A. Color-singlet contributions

The inelastic J/ψ -photoproduction has long been studied in the framework of PQCD and the color-singlet model [1] [15]. The lowest order subprocess at the parton level for $\gamma + p \rightarrow J/\psi + X$ is the γ -gluon fusion at the short distance scale (Fig. 1),

$$\gamma + g \rightarrow (c\bar{c})(^3S_1^{(1)}) + g, \quad (3.1)$$

followed by the long distance process

$$(c\bar{c})(^3S_1^{(1)}) \rightarrow J/\psi, \quad (3.2)$$

at the order of $O(\alpha_s^2 v^3)$ in the nonrelativistic limit. Thus, the production cross section is proportional to the gluon distribution inside the proton. This is why the J/ψ -photoproduction has been advocated as a clean probe for the gluon structure function of a proton in the color-singlet model. Without further details, we show the lowest order color-singlet contribution to J/ψ photoproduction through γ -gluon fusion in the nonrelativistic limit :

$$\overline{|\mathcal{M}(\gamma g \rightarrow J/\psi g)|^2} = \mathcal{N}_1 \frac{\hat{s}^2(\hat{s} - 4M_c^2)^2 + \hat{t}^2(\hat{t} - 4M_c^2)^2 + \hat{u}(\hat{u} - 4M_c^2)^2}{(\hat{s} - 4M_c^2)^2(\hat{t} - 4M_c^2)^2(\hat{u} - 4M_c^2)^2}, \quad (3.3)$$

where

$$\begin{aligned}
z &= \frac{E_\psi}{E_\gamma}|_{\text{lab}} = \frac{p_N \cdot P}{p_N \cdot k}, \\
\hat{s} &= (k + q_1)^2 = xs, \\
\hat{t} &= (P - k)^2 = (z - 1)\hat{s}.
\end{aligned} \quad (3.4)$$

The overall normalization \mathcal{N}_1 is defined as

$$\mathcal{N}_1 = \frac{32}{9} (4\pi\alpha_s)^2 (4\pi\alpha) e_c^2 M_c^3 G_1(J/\psi). \quad (3.5)$$

The parameter $G_1(J/\psi)$, which is defined as

$$G_1(J/\psi) = \frac{\langle J/\psi | \mathcal{O}_1(^3S_1) | J/\psi \rangle}{M_c^2} \quad (3.6)$$

in the NRQCD, is proportional to the probability that a color-singlet $c\bar{c}$ pair in the $^3S_1^{(1)}$ partial wave state to form a physical J/ψ state. It is related with the leptonic decay via

$$\Gamma(J/\psi \rightarrow l^+l^-) = \frac{2}{3} \pi e_c^2 \alpha^2 G_1(J/\psi), \quad (3.7)$$

to the lowest order in α_s . From the measured leptonic decay rate of J/ψ , one can extract

$$G_1(J/\psi) \approx 106 \text{ MeV}, \quad (3.8)$$

Including the radiative corrections of $O(\alpha_s)$ with $\alpha_s(M_c) = 0.27$, it is increased to ≈ 184 MeV. Relativistic corrections tend to increase $G_1(J/\psi)$ further to ~ 195 MeV [10].

The partonic cross section for $\gamma + a \rightarrow J/\psi + b$ is given by

$$\frac{d\hat{\sigma}}{d\hat{t}} = \frac{1}{16\pi\hat{s}^2} \overline{\sum} |\mathcal{M}(\gamma + a \rightarrow J/\psi + b)|^2. \quad (3.9)$$

The double differential cross section is

$$\frac{d^2\sigma}{dzdP_T^2}(\gamma + p(p_N) \rightarrow J/\psi(P, \epsilon) + X) = \frac{xg(x, Q^2)}{z(1-z)} \frac{1}{16\pi\hat{s}^2} \overline{\sum} |\mathcal{M}|^2(\hat{s}, \hat{t}), \quad (3.10)$$

where

$$x = \frac{\hat{s}}{s} = \frac{1}{zs} \left[M_\psi^2 + \frac{P_T^2}{1-z} \right]. \quad (3.11)$$

One has the following constraints for x, z, t and P_T^2 :

$$\frac{M_\psi^2}{s} < x < 1, \quad (3.12)$$

$$-(\hat{s} - M_\psi^2) \leq \hat{t}(=t) \leq 0, \quad (3.13)$$

$$M_\psi^2 \leq \frac{M_\psi^2}{z} + \frac{P_T^2}{z(1-z)} \leq s. \quad (3.14)$$

The z and P_T^2 distributions can be obtained in the following manner :

$$\frac{d\sigma}{dz} = \int_0^{(1-z)(zs-M_\psi^2)} \frac{d^2\sigma}{dzdP_T^2} dP_T^2, \quad (3.15)$$

$$\frac{d\sigma}{dP_T^2} = \int_{z_{\min}}^{z_{\max}} \frac{d^2\sigma}{dzdP_T^2} dz, \quad (3.16)$$

$$z_{\max} = \frac{1}{2s} \left(s + M_\psi^2 + \sqrt{(s - M_\psi^2)^2 - 4sP_T^2} \right), \quad (3.17)$$

$$z_{\min} = \frac{1}{2s} \left(s + M_\psi^2 - \sqrt{(s - M_\psi^2)^2 - 4sP_T^2} \right). \quad (3.18)$$

There are two kinds of corrections to the lowest order result in the color-singlet model, (3.1) : the relativistic corrections of $O(v^2)$ and the PQCD radiative corrections of $O(\alpha_s)$ relative to the lowest order result shown in (3.1). We briefly summarize both types of corrections in the rest of this subsection, since they have to be included in principle for consistency, when one includes the color-octet mechanism in many cases.

The relativistic corrections to the γ -gluon fusion was studied by Jung *et al.* [15]. They found that relativistic corrections are important for high $z > 0.9$ at EMC energy ($\sqrt{s_{\gamma p}} \simeq 14.7$ GeV). Since it mainly affects the high z region only, we neglect the relativistic corrections, keeping in mind that it enhances the cross section at large $z > 0.9$.

The radiative corrections to the J/ψ photoproduction is rather important in practice. This calculation has been done recently in Ref. [16], and the scale dependence of the lowest order result (Q^2 in the structure function in Eq. (3.10)) becomes considerably reduced. For EMC energy region, the K factor is rather large, $K \sim 2$. For HERA, it depends on the cuts in z and P_T^2 . We include the radiative corrections in terms of a K factor suitable to the energy range we consider. Another consequence of the radiative corrections to the color-singlet J/ψ photoproduction is that the PQCD becomes out of control for $z > 0.9$ at EMC energy. For HERA, one gets reasonable results in PQCD when one imposes the following cuts in z and P_T^2 : $z < 0.8$ and $P_T^2 > 1 \text{ GeV}^2$. Thus, it is not too much of sense to talk about the z or p_T distributions for such z region in PQCD. One has to introduce cuts in z as well as in p_T . Following the Ref. [16], we adopt the following sets of cuts :

$$z < 0.9, \quad \text{for EMC}, \quad (3.19)$$

$$0.2 < z < 0.8 \quad \text{for HERA}. \quad (3.20)$$

At HERA energies, the lower cut in $z(z > 0.2)$ is employed in order to reduce backgrounds from the resolved photon process and the b decays into J/ψ . For these cuts, the K factor is approximately $K \simeq 1.8$ both at HERA and the fixed target experiments. We include these radiative corrections to the subprocess (3.1) in Sec. IV A by setting $K \simeq 1.8$.

B. Color-octet contributions to $2 \rightarrow 1$ subprocesses

Let us consider color-octet contributions to the $2 \rightarrow 1$ subprocesses via

$$\gamma(k) + g_a^*(g) \rightarrow (c\bar{c})[{}^{2S+1}L_J^{(8b)}](P), \quad (3.21)$$

followed by $(c\bar{c})_8$ fragmenting into J/ψ with emission of soft gluons. This subprocess occurs at $O(\alpha\alpha_s v^7)$. Here, a, b are color indices for the initial gluon and the final color-octet $c\bar{c}$ state, and we are interested in $S = L = J = 0$ and $S = L = 1, J = 0, 1, 2$. There are 2 diagrams representing the vertex, as shown in Fig. 2. Here we consider the process where only the gluon is off-shell. Following previous convention, we first write the matrix \mathcal{O} related to this effective vertices.

$$\mathcal{O}(P, q) = \frac{ee_c g_s \delta^{ab}}{\sqrt{2}} \left[\not{\epsilon}^\gamma \frac{\not{P} + \not{q} - \not{k} + M_c}{(\frac{P}{2} + q - k)^2 - M_c^2} \not{\epsilon}^{g+} + \not{\epsilon}^g \frac{\not{P} + \not{q} - \not{g} + M_c}{(\frac{P}{2} + q - g)^2 - M_c^2} \not{\epsilon}^\gamma \right]. \quad (3.22)$$

With this matrix \mathcal{O} we can derive the effective vertices for the $\gamma g(c\bar{c})^{2S+1}L_J^{(8)}$ as

$$\mathcal{M}'(^1S_0^{(8)}) = 4i \frac{ee_c g_s}{g^2 - 4M_c^2} \delta^{ab} \epsilon^{\mu\nu\kappa\lambda} \epsilon_\mu^\gamma \epsilon_\nu^g P_\kappa k_\lambda, \quad (3.23)$$

$$\mathcal{M}'(^3S_1^{(8)}) = 0, \quad (3.24)$$

$$\mathcal{M}'(^3P_0^{(8)}) = \frac{2ee_c g_s \delta^{ab}}{\sqrt{3}M_c} \left(\frac{g^2 - 12M_c^2}{g^2 - 4M_c^2} \right) \left(g^{\mu\nu} + 2 \frac{P^\mu k^\nu}{g^2 - 4M_c^2} \right) \epsilon_\mu^\gamma \epsilon_\nu^g, \quad (3.25)$$

$$\begin{aligned} \mathcal{M}'(^3P_1^{(8)}) &= \frac{\sqrt{2}ee_c g_s \delta^{ab}}{M_c^2 (g^2 - 4M_c^2)} \\ &\times \left(g^2 \epsilon^{\mu\nu\alpha\tau} + 2k_\kappa \frac{g^2 (P^\mu \epsilon^{\nu\alpha\kappa\tau} - P^\nu \epsilon^{\mu\alpha\kappa\tau}) + 4g^\nu M_c^2 \epsilon^{\mu\alpha\kappa\tau}}{g^2 - 4M_c^2} \right) \epsilon_\alpha(J_z) \epsilon_\mu^\gamma \epsilon_\nu^g P_\tau, \end{aligned} \quad (3.26)$$

$$\mathcal{M}'(^3P_2^{(8)}) = \frac{16ee_c g_s \delta^{ab}}{(g^2 - 4M_c^2)} M_c \left(g^{\mu\alpha} g^{\nu\beta} + 2k^\alpha \frac{k^\beta g^{\mu\nu} + P^\mu g^{\nu\beta} - k^\nu g^{\mu\beta}}{g^2 - 4M_c^2} \right) \epsilon_{\alpha\beta}(J_z) \epsilon_\mu^\gamma \epsilon_\nu^g. \quad (3.27)$$

Since J/ψ can be produced via the $2 \rightarrow 1$ subprocesses with this effective vertices we can obtain the $2 \rightarrow 1$ color octet contribution by using the following average squared amplitudes as ²

$$\overline{\sum} |\mathcal{M}'(^1S_0^{(8)})|^2 = 2(ee_c g_s)^2, \quad (3.28)$$

$$\overline{\sum} |\mathcal{M}'(^3S_1^{(8)})|^2 = 0, \quad (3.29)$$

$$\overline{\sum} |\mathcal{M}'(^3P_0^{(8)})|^2 = \frac{6}{M_c^2} (ee_c g_s)^2, \quad (3.30)$$

$$\overline{\sum} |\mathcal{M}'(^3P_1^{(8)})|^2 = 0, \quad (3.31)$$

$$\overline{\sum} |\mathcal{M}'(^3P_2^{(8)})|^2 = \frac{8}{M_c^2} (ee_c g_s)^2. \quad (3.32)$$

The photoproduction cross section of the J/ψ production via $2 \rightarrow 1$ process can be obtained from (2.42), assuming heavy quark spin symmetry :

$$\begin{aligned} \sigma(\gamma + p \rightarrow (c\bar{c})^{(8)} \rightarrow \psi) \\ = \frac{7\pi(ee_c g_s)^2}{64M_c^5} [xf_{g/p}(x)]_{x=4M_c^2/s} \left(\frac{\langle 0|\mathcal{O}^\psi(^3P_0^{(8)})|0\rangle}{M_c^2} + \frac{\langle 0|\mathcal{O}^\psi(^1S_0^{(8)})|0\rangle}{7} \right). \end{aligned} \quad (3.33)$$

Since $\hat{\sigma} \propto \delta(1-z)$, this $2 \rightarrow 1$ color-octet subprocesses contribute to the elastic peak in the J/ψ -photoproductions. It is timely to recall that the color-singlet model with relativistic corrections still underestimate the cross section for $z \geq 0.9$ by an appreciable amount [15]. As $z \rightarrow 1$, the final state gluon in the γ -gluon fusion becomes softer and softer, although this does not cause any infrared divergence in the transition matrix element. Therefore,

²Our results agree with those obtained in Refs. [12] [13]. Note, however, that our convention of the invariant matrix is different from theirs.

it would be more meaningful to factorize the effect of this final soft gluon into the color-octet matrix elements, $\langle O_8^\psi(^1S_0) \rangle$ and $\langle O_8^\psi(^3P_J) \rangle$. The color-octet 1S_0 and 3P_J states might reduce the gap between the color-singlet prediction and the experimental value of $d\sigma/dz$ for $0.9 \leq z \leq 1$.

C. Color-octet contributions to the $2 \rightarrow 2$ subprocesses

The color-octet $2 \rightarrow 1$ subprocess (3.21) considered in the previous subsection not only contribute to the elastic peak of the J/ψ photoproduction, but it also contributes to the resolved photon processes at $O(\alpha\alpha_s^2v^7)$, shown in Fig. 3, where the initial partons can be either gluon or light quarks ($q = u, d, s$). These diagrams are suppressed by v^4 but enhanced by $1/\alpha_s$, relative to the resolved photon process in the color-singlet model. Also, the jet structures from Fig. 3 are different from that from the resolved photon process in the color-singlet model. They can enhance the high- $p_T J/\psi$'s, which might be relevant to HERA energy. This can be a background to the determination of gluon distribution function of a proton, if the cross section is appreciable. The resolved photon process in the color-singlet model is dominant over the γ -gluon fusion in the lower z region, $z < 0.2$, and it can be discarded by a suitable cut on z . Since the color-octet contribution to the resolved photon process has not been studied in the literature, we address this issue in the following. When one considers Fig. 3, one has to include Fig. 1 with $(c\bar{c})_8$ simultaneously, since both are the same order of $O(\alpha\alpha_s^2v^7)$. This diagram is the same as the color-singlet case except for the color factor of the $(c\bar{c})$ state.

It is straightforward, although lengthy, to calculate the amplitudes for the processes shown in Figs. 1 and 3. Using REDUCE in order to the spinor algebra in a symbolic manner, we can get the averaged \mathcal{M} squared for various $2 \rightarrow 2$ processes. Since the full expressions are rather involved, they are shown in Appendix A.

Another color-octet $(c\bar{c})(^3S_1^{(8)})$ contribution to the J/ψ -photoproductions comes from the Compton scattering type subprocesses (see Fig. 4) :

$$\gamma(k, \epsilon) + q(p_1) \rightarrow (c\bar{c})(^3S_1^{(8a)})(P, \epsilon^*) + q(p_2), \quad (3.34)$$

where P and ϵ^* are the four momentum and the polarization vector of the 3S_1 color-octet state, and a is its color index. This subprocess, if important, can be a background to the determination of the gluon distribution function in a proton, since it is initiated by light quarks. From the naive power counting, however, we infer this subprocess occurs at $O(\alpha\alpha_s^2)$ in the coupling constant expansion, and also suppressed by v^4 compared to the color-singlet contribution (3.1) due to its color-octet nature. Thus, this subprocess is expected to be negligible.

One can actually quantify this argument by explicitly evaluating the Feynman diagrams shown in Fig. 4. The effective vertex for $q\bar{q} \rightarrow (c\bar{c})(^3S_1^{(8a)})$ is given by (Fig. 5) [4]

$$\mathcal{M}'(q(p_1)\bar{q}(p_2) \rightarrow (c\bar{c})(^3S_1^{(8a)})) = \frac{4\pi\alpha_s}{2M_c} \bar{v}(p_2)\gamma^\mu T^a u(p_1) \epsilon_\mu^*(p_1 + p_2, S_z), \quad (3.35)$$

where ϵ_μ^* is the polarization of the produced spin-1 color octet object. Using this effective vertex, one can calculate the amplitude for the Feynman diagrams shown in Fig. 4 :

$$\mathcal{M}'(\gamma q \rightarrow (c\bar{c})(^3S_1^{(8a)})q) = -\frac{g_s^2 ee_q}{2M_c} \bar{u}(p_2) \left[\not{\epsilon}^*(P, S_z) T_a \frac{(k + p_1 + M_c)}{(k + p_1)^2 - M_c^2} \not{\epsilon}_\gamma + \not{\epsilon}_\gamma \frac{(p_1 - P + M_c)}{(p_1 - P)^2 - M_c^2} \not{\epsilon}^*(P, S_z) T_a \right] u(p_1). \quad (3.36)$$

where ee_q is the electric charge of the light quark inside proton ($q = u, d, s$). The averaged \mathcal{M}^2 for the color-octet 3S_1 state is given by

$$\overline{|\mathcal{M}'(\gamma q \rightarrow (c\bar{c})(^3S_1^{(8)})q)|^2} = -\frac{2}{3M_c^2} (g_s^2 ee_q)^2 \left(\frac{\hat{s}}{\hat{u}} + \frac{\hat{u}}{\hat{s}} + 8 \frac{M_c^2 \hat{t}}{\hat{s}\hat{u}} \right). \quad (3.37)$$

This completes our discussions on the color-octet $2 \rightarrow 2$ subprocess for J/ψ photoproductions.

IV. NUMERICAL RESULTS

A. J/ψ photoproductions at fixed targets and HERA

Now, we are ready to show the numerical results using the analytic expressions obtained in the previous section. Let us first summarize the input parameters and the structure functions we will use in the following. The results are quite sensitive to the numerical values of α_s and m_c and the factorization scale Q . We shall use $\alpha_s(M_c^2) = 0.3$, $m_c = 1.48$ GeV and $Q^2 = (2m_c)^2$. For the structure functions, we use the most recent ones, MRSA [17] and CTEQ3M [18], which incorporate the new data from HERA [19], on the lepton asymmetry in W -boson production [20] and on the difference in Drell-Yan cross sections from proton and neutron targets [21]. For the $2 \rightarrow 1$, we show results using both structure functions. For the $2 \rightarrow 2$ case, we show the results with the CTEQ3M structure functions only, since the MRSA structure functions yield more or less the same results within $\sim 10\%$ or so.

Let us first consider the J/ψ photoproduction via the color-octet $2 \rightarrow 1$ subprocess considered in Sec. III B. Since the subprocess cross section (3.33) vanishes except at $z = 1$, one can infer that it contributes to the J/ψ photoproductions in the forward direction ($z \sim 1, P_T^2 \simeq 0$). In Figs. 6 (a) and (b), we show the J/ψ photoproduction cross section in the forward direction as well as the data from the fixed target experiments and the preliminary data from H1 at HERA, respectively. In each case, the upper and the lower curves define the region allowed by the relation (1.4) for two color-octet matrix elements, $\langle 0 | O_8^\psi(^3S_1) | 0 \rangle$ and $\langle 0 | O_8^\psi(^3P_0) | 0 \rangle$. In case of fixed target experiments, it is usually characterized by $z > 0.9$, with the remainder being associated with the inelastic J/ψ photoproduction. According to this criterion, the experimental value of $\sigma_{\text{exp}}(\gamma + p \rightarrow J/\psi + X)$ contains contributions from inelastic production of J/ψ 's. Thus, the data should lie above the predictions from the color-octet $2 \rightarrow 1$ subprocess, (3.21). Fig. 6 (a) shows that the situation is opposite to this expectation. Color-octet contributions are larger than the data, which indicates that the numerical values of the color-octet matrix elements are probably too large. At HERA, one has the elastic J/ψ photoproduction data, which can be identified with the color-octet $2 \rightarrow 1$ subprocess. By saturating the relation (1.4) by either color-octet matrix element, we

get the J/ψ photoproduction cross section in the forward direction (Fig. 6 (b)). We observe again that the color-octet contribution with (1.4) overestimates the cross section by a large amount. This disagreement can arise from two sources : (i) the radiative corrections to $p\bar{p} \rightarrow J/\psi + X$, which were ignored in Ref. [5] is important, and/or (ii) the heavy quark spin symmetry for $\langle 0|O_8^\psi(^3P_J)|0\rangle \approx (2J+1)\langle 0|O_8^\psi(^3P_0)|0\rangle$ may not be a good approximation. Although the heavy quark spin symmetry relation is used quite often in heavy quarkonium physics, it may be violated by a considerable amount [10].

Recently, Fleming *et al.* performed the χ^2 fit to the available fixed target experiments and the HERA data independently, and found that

$$\langle 0|O_8^\psi(^1S_0)|0\rangle + \frac{7}{M_c^2} \langle 0|O_8^\psi(^3P_0)|0\rangle = (0.020 \pm 0.001) \text{ GeV}^3, \quad (4.1)$$

using the MRSA⁽¹⁾, and CTEQ3M structure functions with $\alpha_s(2M_c) = 0.26$ and $M_c = 1.5$ GeV. This determination is not compatible with the relation (1.4), since the resulting $\langle O_8(^3P_0)\rangle$ is negative. This is another way to say that the determination of the color-octet matrix elements from the J/ψ productions at the Tevatron may not be that reliable. In fact, this is not very surprising, since the radiative corrections to the lowest-order color-singlet contributions to J/ψ hadronic productions are not included yet.

Next, we consider J/ψ photoproductions through $2 \rightarrow 2$ parton-level subprocesses. As discussed at the end of Sec. III A, the PQCD corrections to the lowest order $\gamma + g \rightarrow J/\psi + g$ is not under proper control for $z > 0.9$. Therefore, we impose a cut $z < 0.9$ at EMC energy, $\sqrt{s_{\gamma p}} = 14.7$ GeV, and at HERA with $\sqrt{s_{\gamma p}} = 100$ GeV, we impose cuts on z and P_T^2 [16] :

$$0.2 < z < 0.8, \quad P_T^2 > 1 \text{ GeV}^2.$$

In both cases, we set $K \simeq 1.8$.

In Figs. 7 (a) and (b), we show the $d\sigma/dz$ distributions of J/ψ at EMC (NMC) and HERA along with the corresponding data. In both cases, the color-octet 3S_1 contribution (Compton scattering type) is negligible in most regions of z , and thus can be safely neglected. The thick dashed and the thin dashed curves correspond to the cases where the relation (1.4) is saturated by $O_8(^3P_J)$ and $O_8(^1S_0)$, respectively. The thick and the thin solid curves represent the sum of the color-singlet and the color-octet contributions, in case that the relation (1.4) is saturated by $\langle 0|O_8^\psi(^1S_0)|0\rangle$ and $\langle 0|O_8^\psi(^3P_0)|0\rangle$, respectively. In either case, we observe that the color-octet 1S_0 and 3P_J contributions begin to dominate the color-singlet contributions for $z > 0.6$, and become too large for high z region considering we have not added the enhancements at high z due to the relativistic corrections. Thus, this behavior of rapid growing at high z does not agree with the data points at EMC and HERA, if we adopt the determination (1.4) by Cho and Leibovich [5].

In Figs. 8 (a) and (b), we show the P_T^2 distributions of J/ψ at EMC and HERA, respectively. We find that the color-octet contributions through $2 \rightarrow 2$ subprocesses become dominant over the color-singlet contributions for most P_T^2 region. Also, the color-octet contributions from 1S_0 and 3P_J are more important than the charm quark fragmentation considered by Godbole *et al.* [22]. However, this situation may be due to the overestimated color-octet matrix elements as alluded in the previous paragraph.

In Fig. 9, we show the inelastic J/ψ photoproduction cross section as a function of $\sqrt{s_{\gamma p}}$ with the cut, $z < 0.8$ and $P_T^2 > 1 \text{ GeV}^2$. Again, the color-octet 3S_1 contribution is too small,

and thus not shown in the Figure. Here again, the color-octet 1S_0 and 3P_J contributions via $2 \rightarrow 2$ subprocesses (Fig. 3) dominate the color-singlet contribution, if the relation (1.4) is imposed. Although the total seems to be in reasonable agreement with the preliminary H1 data, direct comparison may be meaningful only if the cascade J/ψ 's from b decays have been subtracted out. There are also considerable amount of uncertainties coming from M_c and α_s . Therefore, it is sufficient to say that the color-octet 1S_0 and 3P_J state dominate the singlet contribution to J/ψ photoproduction, if the relation (1.4) is imposed.

B. Digression on $B \rightarrow J/\psi + X$

Finding that the color-octet matrix elements determined from J/ψ productions at the Tevatron seem to be too large in case of J/ψ photoproductions at fixed target experiments and HERA, it is timely to consider the color-octet contributions to inclusive B meson decays into $J/\psi + X$ again. In Ref. [10], a new factorization formula is derived for $B \rightarrow J/\psi + X$:

$$\begin{aligned} \Gamma(B \rightarrow J/\psi + X) = & \left(\frac{\langle 0|O_1^{J/\psi}(^3S_1)|0\rangle}{3M_c^2} - \frac{\langle 0|P_1^{J/\psi}(^3S_1)|0\rangle}{9M_c^4} \right) (2C_+ - C_-)^2 \left(1 + \frac{8M_c^2}{M_b^2} \right) \hat{\Gamma}_0 \\ & + \frac{3\langle 0|O_8^{J/\psi}(^1S_0)|0\rangle}{2M_c^2} (C_+ + C_-)^2 \hat{\Gamma}_0 \\ & + \frac{\langle 0|O_8^{J/\psi}(^3P_1)|0\rangle}{M_c^4} (C_+ + C_-)^2 \left(1 + \frac{8M_c^2}{M_b^2} \right) \hat{\Gamma}_0, \end{aligned} \quad (4.2)$$

with

$$\hat{\Gamma}_0 \equiv |V_{cb}|^2 \left(\frac{G_F^2}{144\pi} \right) M_b^3 M_c \left(1 - \frac{4M_c^2}{M_b^2} \right)^2. \quad (4.3)$$

Two numbers $C_+(M_b) \approx 0.87$ and $C_-(M_b) \approx 1.34$ are the Wilson coefficients of the $|\Delta B| = 1$ effective weak Hamiltonian. Using the relation (1.4), we estimate the above branching ratio to be (for $\alpha_s(M_\psi^2) = 0.28$ in Ref. [10])

$$(0.42\% \times 12.8) < B(B \rightarrow J/\psi + X) < (0.42\% \times 13.8) \quad (4.4)$$

which is larger than the recent CLEO data by an order of magnitude ³:

$$B_{\text{exp}}(B \rightarrow J/\psi + X) = (0.80 \pm 0.08)\%. \quad (4.6)$$

³Even if we use the new determination (4.1) by Fleming *et al.* [13], we still get a large branching ratio :

$$(0.42\% \times 3.45) < B(B \rightarrow J/\psi + X) < (0.42\% \times 5.45), \quad (4.5)$$

although the discrepancy gets milder than the case (4.4).

The situation is the same for $B \rightarrow \psi' + X$. This is problematic, unless this large color-octet contributions are canceled by the color-singlet contributions of higher order in $O(\alpha_s)$ which were not included in Ref. [10]. If there are no such fortuitous cancelations among various color-octet and the color-singlet contributions, this disaster could be attributed to the relation (1.4) being too large compared to the naive velocity scaling rule in NRQCD, as noticed in Ref. [5]. It seems to be crucial to include the higher order corrections of $O(\alpha_s^4)$ for the color-singlet J/ψ productions at the Tevatron, which is still lacking in the literature.

V. CONCLUSION

In summary, we considered the color-octet contributions to (i) the subprocess $\gamma + p \rightarrow J/\psi + X$ through $\gamma g \rightarrow (c\bar{c})_8(^1S_0$ and $^3P_J)$ and the subsequent evolution of $(c\bar{c})_8$ into a physical J/ψ with $z \approx 1$ and $P_T^2 \approx 0$, (ii) the subprocesses $\gamma + g(\text{or } q) \rightarrow (c\bar{c})_8(^1S_0$ or $^3P_J) + g(\text{or } q)$. These are compared with (i) the measured J/ψ photoproduction cross section in the forward direction, and (ii) the z distributions of J/ψ at EMC and HERA, and the preliminary result on the inelastic J/ψ photoproduction total cross section at HERA. One finds that the relation (1.4) color-octet lead to too large contributions of the color-octet 1S_0 and 3P_J states to the above observables. Especially, the first two observables contradict the observation. This is also against the naive expectation that the color-octet contribution may not be prominent as in the case of the J/ψ hadroproductions, since they are suppressed by v^4 (although enhanced by one power of α_s) relative to the color-singlet contribution. It is also pointed out that the same is true of the process $B \rightarrow J/\psi + X$, in which the relation (1.4) predicts its branching ratio to be too large by an order of magnitude compared with the data.

Therefore, one may conclude that the color-octet matrix elements involving $c\bar{c}_8(^1S_0, ^3P_J)$ might be overestimated by an order of magnitude. Since the relation (1.4) has been extracted by fitting the J/ψ production at the Tevatron to the lowest order color-singlet and the color-octet contributions, it may be changed when one considers the radiative corrections to the lowest order color-singlet contributions.

While we were finishing our work, there appeared two papers considering the same subject [12] [13]. Our results agree with these two works where they overlap.

ACKNOWLEDGMENTS

This work was supported in part by KOSEF through CTP at Seoul National University. P.K. is supported in part by the Basic Science Research Program, Ministry of Education, 1995, Project No. BSRI-95-2425, and in part by NON DIRECTED RESEARCH FUND, Korea Research Foundations (1995).

**APPENDIX A: THE INVARIANT AMPLITUDE SQUARED FOR THE $2 \rightarrow 2$
SUBPROCESSES CONSIDERED IN SEC. III.C.**

In this Appendix, we give explicit expressions for the invariant amplitude squared for the color-octet $2 \rightarrow 2$ subprocesses shown in Figs. 1 and 3. The results were obtained using the symbolic manipulations with the aid of REDUCE package. Without further details, we show the results :

$$\begin{aligned} \overline{\sum} |\mathcal{M}|^2(\gamma + g \rightarrow (c\bar{c}) ({}^1S_0^{(8)}) + g) &= \frac{6su(ee_c g_s^2)^2}{\hat{t}(\hat{s} + \hat{t})^2(\hat{t} + \hat{u})^2(\hat{u} + \hat{s})^2} \\ &\times \left[4(\hat{s} + \hat{u})^4 - 8\hat{s}\hat{u}(\hat{s} + \hat{u})^2 + 5\hat{s}^2\hat{u}^2 + 2\hat{t}(\hat{s} + \hat{u})(4(\hat{s} + \hat{u})^2 + \hat{s}\hat{u}) \right. \\ &\quad \left. + \hat{t}^2(13(\hat{s} + \hat{u})^2 + 2\hat{s}\hat{u}) + 10\hat{t}^3(\hat{s} + \hat{u}) + 5\hat{t}^4 \right], \end{aligned} \quad (\text{A1})$$

$$\begin{aligned} \overline{\sum} |\mathcal{M}'|^2(\gamma + g \rightarrow (c\bar{c}) ({}^3P_0^{(8)}) + g) &= \frac{2\hat{s}\hat{u}(ee_c g_s^2)^2}{M_c^2 \hat{t}(\hat{s} + \hat{t})^4(\hat{t} + \hat{u})^4(\hat{u} + \hat{s})^4} \\ &\times \left[9\hat{s}^2\hat{u}^2(\hat{s} + \hat{u})^2 \left(4(\hat{s} + \hat{u})^4 - 8\hat{s}\hat{u}(\hat{s} + \hat{u})^2 + 5\hat{s}^2\hat{u}^2 \right) \right. \\ &\quad + 12\hat{t}\hat{s}\hat{u}(\hat{s} + \hat{u}) \left(6(\hat{s} + \hat{u})^6 - 6\hat{s}\hat{u}(\hat{s} + \hat{u})^4 + 5\hat{s}^2\hat{u}^2(\hat{s}^2 + 3\hat{s}\hat{u} + \hat{u}^2) \right) \\ &\quad + 2\hat{t}^2 \left(18(\hat{s} + \hat{u})^8 + 72\hat{s}\hat{u}(\hat{s} + \hat{u})^6 - 17\hat{s}^2\hat{u}^2(\hat{s} + \hat{u})^4 + 150\hat{s}^3\hat{u}^3(\hat{s} + \hat{u})^2 + 10\hat{s}^4\hat{u}^4 \right) \\ &\quad + 4\hat{t}^3(\hat{s} + \hat{u}) \left(36(\hat{s} + \hat{u})^6 + 51\hat{s}\hat{u}(\hat{s} + \hat{u})^4 + 95\hat{s}^2\hat{u}^2(\hat{s} + \hat{u})^2 + 56\hat{s}^3\hat{u}^3 \right) \\ &\quad + \hat{t}^4 \left(305(\hat{s} + \hat{u})^6 + 380\hat{s}\hat{u}(\hat{s} + \hat{u})^4 + 502\hat{s}^2\hat{u}^2(\hat{s} + \hat{u})^2 + 48\hat{s}^3\hat{u}^3 \right) \\ &\quad + 4\hat{t}^5(\hat{s} + \hat{u}) \left(116(\hat{s} + \hat{u})^4 + 113\hat{s}\hat{u}(\hat{s} + \hat{u})^2 + 58\hat{s}^2\hat{u}^2 \right) \\ &\quad + 2\hat{t}^6 \left(257(\hat{s} + \hat{u})^4 + 142\hat{s}\hat{u}(\hat{s} + \hat{u})^2 + 20\hat{s}^2\hat{u}^2 \right) \\ &\quad + 12\hat{t}^7(\hat{s} + \hat{u})(31\hat{s}^2 + 70\hat{s}\hat{u} + 31\hat{u}^2) \\ &\quad \left. + \hat{t}^8(149\hat{s}^2 + 314\hat{s}\hat{u} + 149\hat{u}^2) + 28\hat{t}^9(\hat{s} + \hat{u}) + 4\hat{t}^{10} \right], \end{aligned} \quad (\text{A2})$$

$$\begin{aligned} \overline{\sum} |\mathcal{M}'|^2(\gamma + g \rightarrow (c\bar{c}) ({}^3P_1^{(8)}) + g) &= \frac{6(ee_c g_s^2)^2}{M_c^2 (\hat{s} + \hat{t})^4(\hat{t} + \hat{u})^4(\hat{u} + \hat{s})^4} \\ &\times \left[5\hat{u}^4\hat{s}^4(\hat{s} - \hat{u})^2(\hat{s} + \hat{u}) \right. \\ &\quad + \hat{t}\hat{s}^3\hat{u}^3 \left(12(\hat{s}^4 + \hat{u}^4) + 21\hat{s}\hat{u}(\hat{s}^2 + \hat{u}^2) + 8\hat{s}^2\hat{u}^2 \right) \\ &\quad + 2\hat{t}^2\hat{s}^2\hat{u}^2(\hat{s} + \hat{u}) \left(11(\hat{s}^4 + \hat{u}^4) + 36\hat{s}\hat{u}(\hat{s}^2 + \hat{u}^2) + 30\hat{s}^2\hat{u}^2 \right) \\ &\quad + 2\hat{t}^3\hat{s}\hat{u} \left(6(\hat{s}^6 + \hat{u}^6) + 61\hat{s}\hat{u}(\hat{s}^4 + \hat{u}^4) + 158\hat{s}^2\hat{u}^2(\hat{s}^2 + \hat{u}^2) + 194\hat{s}^3\hat{u}^3 \right) \\ &\quad + \hat{t}^4(\hat{s} + \hat{u}) \left(5(\hat{s}^6 + \hat{u}^6) + 66\hat{s}\hat{u}(\hat{s}^4 + \hat{u}^4) + 217\hat{s}^2\hat{u}^2(\hat{s}^2 + \hat{u}^2) + 248\hat{s}^3\hat{u}^3 \right) \\ &\quad + \hat{t}^5 \left(17(\hat{s}^6 + \hat{u}^6) + 124\hat{s}\hat{u}(\hat{s}^4 + \hat{u}^4) + 265\hat{s}^2\hat{u}^2(\hat{s}^2 + \hat{u}^2) + 296\hat{s}^3\hat{u}^3 \right) \\ &\quad + 2\hat{t}^6(\hat{s} + \hat{u}) \left(11(\hat{s}^4 + \hat{u}^4) + 32\hat{s}\hat{u}(\hat{s}^2 + \hat{u}^2) + 14\hat{s}^2\hat{u}^2 \right) \\ &\quad + 2\hat{t}^7 \left(7(\hat{s}^4 + \hat{u}^4) + 12\hat{s}\hat{u}(\hat{s}^2 + \hat{u}^2) + 6\hat{s}^2\hat{u}^2 \right) \\ &\quad \left. + \hat{t}^8(\hat{s} + \hat{u}) \left(5(\hat{s}^2 + \hat{u}^2) - 2\hat{s}\hat{u} \right) + \hat{t}^9(\hat{s}^2 + \hat{u}^2) \right], \end{aligned} \quad (\text{A3})$$

$$\begin{aligned}
\overline{\sum} |\mathcal{M}'|^2(\gamma + g \rightarrow (c\bar{c}) ({}^3P_2^{(8)}) + g) &= \frac{2(ee_c g_s^2)^2}{M_c^2 \hat{t}(\hat{s} + \hat{t})^4(\hat{t} + \hat{u})^4(\hat{u} + \hat{s})^4} \\
&\times \left[12\hat{u}^3\hat{s}^3(\hat{s} + \hat{u})^2 \left(4(\hat{s}^4 + \hat{u}^4) + 8\hat{s}\hat{u}(\hat{s}^2 + \hat{u}^2) + 13\hat{s}^2\hat{u}^2 \right) \right. \\
&\quad + 3\hat{t}\hat{s}^2\hat{u}^2(\hat{s} + \hat{u}) \left(32(\hat{s}^6 + \hat{u}^6) + 144\hat{s}\hat{u}(\hat{s}^4 + \hat{u}^4) + 277\hat{s}^2\hat{u}^2(\hat{s}^2 + \hat{u}^2) + 350\hat{s}^3\hat{u}^3 \right) \\
&\quad + \hat{t}^2\hat{s}\hat{u} \left(48(\hat{s}^8 + \hat{u}^8) + 576\hat{s}\hat{u}(\hat{s}^6 + \hat{u}^6) + 1888\hat{s}^2\hat{u}^2(\hat{s}^4 + \hat{u}^4) \right. \\
&\quad \quad \left. + 3395\hat{s}^3\hat{u}^3(\hat{s}^2 + \hat{u}^2) + 4080\hat{s}^4\hat{u}^4 \right) \\
&\quad + 4\hat{t}^3\hat{s}\hat{u}(\hat{s} + \hat{u}) \left(60(\hat{s}^6 + \hat{u}^6) + 333\hat{s}\hat{u}(\hat{s}^4 + \hat{u}^4) + 646\hat{s}^2\hat{u}^2(\hat{s}^2 + \hat{u}^2) + 804\hat{s}^3\hat{u}^3 \right) \\
&\quad + 4\hat{t}^4\hat{s}\hat{u} \left(142(\hat{s}^6 + \hat{u}^6) + 676\hat{s}\hat{u}(\hat{s}^4 + \hat{u}^4) + 1398\hat{s}^2\hat{u}^2(\hat{s}^2 + \hat{u}^2) + 1733\hat{s}^3\hat{u}^3 \right) \\
&\quad + \hat{t}^5(\hat{s} + \hat{u}) \left(9(\hat{s}^6 + \hat{u}^6) + 818\hat{s}\hat{u}(\hat{s}^4 + \hat{u}^4) + 2295\hat{s}^2\hat{u}^2(\hat{s}^2 + \hat{u}^2) + 3028\hat{s}^3\hat{u}^3 \right) \\
&\quad + \hat{t}^6 \left(21(\hat{s}^6 + \hat{u}^6) + 716\hat{s}\hat{u}(\hat{s}^4 + \hat{u}^4) + 2163\hat{s}^2\hat{u}^2(\hat{s}^2 + \hat{u}^2) + 2944\hat{s}^3\hat{u}^3 \right) \\
&\quad + 2\hat{t}^7(\hat{s} + \hat{u}) \left(3(\hat{s}^4 + \hat{u}^4) + 136\hat{s}\hat{u}(\hat{s}^2 + \hat{u}^2) + 206\hat{s}^2\hat{u}^2 \right) \\
&\quad - 2\hat{t}^8 \left(9(\hat{s}^4 + \hat{u}^4) + 14\hat{s}\hat{u}(\hat{s}^2 + \hat{u}^2) + 12\hat{s}^2\hat{u}^2 \right) \\
&\quad \left. - \hat{t}^9(\hat{s} + \hat{u})(3\hat{s} + 5\hat{u})(5\hat{s} + 3\hat{u}) - \hat{t}^{10}(3\hat{s}^2 + 8\hat{s}\hat{u} + 3\hat{u}^2) \right], \tag{A4}
\end{aligned}$$

$$\overline{\sum} |\mathcal{M}'|^2(\gamma + q \rightarrow (c\bar{c}) ({}^1S_0^{(8)}) + q) = -\frac{16}{3}(ee_c g_s^2)^2 \frac{\hat{s}^2 + \hat{u}^2}{\hat{t}(\hat{s} + \hat{u})^2}, \tag{A5}$$

$$\overline{\sum} |\mathcal{M}'|^2(\gamma + q \rightarrow (c\bar{c}) ({}^3P_0^{(8)}) + q) = -\frac{16}{9}(ee_c g_s^2)^2 \frac{(\hat{s}^2 + \hat{u}^2)(\hat{t} - 12M_c^2)^2}{\hat{t}(\hat{s} + \hat{u})^4 M_c^2}, \tag{A6}$$

$$\overline{\sum} |\mathcal{M}'|^2(\gamma + q \rightarrow (c\bar{c}) ({}^3P_1^{(8)}) + q) = -\frac{32}{3}(ee_c g_s^2)^2 \frac{(\hat{s}^2 + \hat{u}^2)\hat{t} + 16M_c^2\hat{s}\hat{u}}{(\hat{s} + \hat{u})^4 M_c^2}, \tag{A7}$$

$$\begin{aligned}
\overline{\sum} |\mathcal{M}'|^2(\gamma + q \rightarrow (c\bar{c}) ({}^3P_2^{(8)}) + q) &= \\
&-\frac{32}{9}(ee_c g_s^2)^2 \frac{(\hat{s} + \hat{u})^2(\hat{t}^2 + 96M_c^4) - 2\hat{s}\hat{u}((\hat{s} + \hat{u} + 4M_c^2)^2 + 8M_c^2(\hat{s} + \hat{u}))}{\hat{t}(\hat{s} + \hat{u})^4 M_c^2}. \tag{A8}
\end{aligned}$$

Here, the $e_c = 2/3$ and we have summed over the electric charges of light quarks ($q = u, d, s$) in the above expressions, assuming $m_q = 0$.

REFERENCES

- [1] E.L. Berger and D. Jones, Phys. Rev. **D 23**, 1521 (1981).
- [2] M. Mangano, CDF Collaboration, presented at the 27th International Conference on High Energy Physics, Glasgow, July (1994), and references therein.
- [3] E. Braaten and S. Fleming, Northwestern University Preprint, NUHEP-TH-94-26 (1994).
- [4] P. Cho and A.K. Leibovich, CIT Preprint, CALT-68-1988 (1995).
- [5] P. Cho and A.K. Leibovich, CIT Preprint, CALT-68-2026 (1995).
- [6] The CDF collaboration, Fermilab-Conf-94/221-E (1994).
- [7] S. Fleming and I. Maksymyk, MADPH-95-922, UTTG-13-95, hep-oh/9512320 (1995).
- [8] P. Cho and M.B. Wise, Phys. Lett. **B346**, 129 (1995).
- [9] E. Braaten and Yu-Qi Chen, NUHEP-TH-95-9, hep-ph/9508373 (1995).
- [10] P. Ko, J. Lee and H.S. Song, Phys. Rev. **D 53**, 1409 (1996).
- [11] K. Cheung, W.-Y. Keung and T.C. Yuan, Fermiab-Pub-95/300-T (1995) ; P. Cho, CALT 68-2020 (1995).
- [12] M. Cacciari and M. Krämer, DESY 96-005, hep-ph/9601276 (1996).
- [13] J. Amundson, S. Fleming and I. Maksymyk, UTTG-10-95, MADTH-95-914, hep-ph/9601298 (1996)
- [14] G.T. Bodwin, E. Braaten and G.P. Lepage, Phys. Rev. **D 51**, 1125 (1995).
- [15] H. Jung, D. Krucker, C. Greub and D. Wyler, Z. Phys. **C 60**, 721 (1993).
- [16] M. Krämer, DESY 95-155 (1995).
- [17] A.D. Martin, R.G. Roberts and W.J. Stirling, Phys. Rev. **D 50**, 6734 (1994).
- [18] H. Lai *et al.*, Phys. Rev. **D 51**, 4763 (1995).
- [19] ZEUS Collaboration, Phys. Lett. **B 316**, 412 (1993) ; H1 Collaboration, Nucl. Phys. **B 407**, 515 (1993).
- [20] CDF Collaboration, F. Abe *et al.*, Phys. Rev. Lett. **74**, 850 (1995).
- [21] NA51 Collaboration, A.Baldit *et al.*, Phys. Lett. **B 332**, 244 (1994).
- [22] R. M. Godbole, D. P. Roy and K. Sridhar, hep-ph/9511433 (1995).

FIGURE CAPTIONS

Fig.1 Feynman diagrams for the color-singlet and the color-octet subprocess $\gamma + g \rightarrow (c\bar{c})_{1,8}(^3S_1) + g$.

Fig.2 Feynman diagrams for the color-octet subprocess $\gamma + g \rightarrow (c\bar{c})_8(^1S_0 \text{ or } ^3P_J)$.

Fig.3 Feynman diagrams for the color-octet contribution to the resolved photon $\gamma + g(\text{or } q) \rightarrow (c\bar{c})_8(^1S_0 \text{ or } ^3P_J) + g(\text{or } q)$.

Fig.4 Feynman diagrams for the color-octet $2 \rightarrow 2$ subprocess, $\gamma + q \rightarrow (c\bar{c})_8(^3S_1) + q$ with $q = u, d, s$.

Fig.5 A Feynman diagram for $q\bar{q} \rightarrow (c\bar{c})_8(^3S_1)$.

Fig.6(a) The cross sections for $\gamma + p \rightarrow J/\psi + X$ in the forward direction at the fixed target experiments as a function of E_γ . The solid and the dashed curves were obtained using the CTEQ3M and the MRSA structure functions. Here, TOT_s is the $^1S_0^{(8)}$ saturated curve and TOT_p is the $^3P_J^{(8)}$ saturated one.

Fig.6(b) The cross sections for $\gamma + p \rightarrow J/\psi + X$ in the forward direction at HERA as a function of the square root of $s_{\gamma p}$. The solid and the dashed curves were obtained using the CTEQ3M and the MRSA structure functions. Here, TOT_s is the $^1S_0^{(8)}$ saturated curve and TOT_p is the $^3P_J^{(8)}$ saturated one.

Fig.7(a) The differential cross sections $d\sigma/dz$ for $\gamma + p \rightarrow J/\psi + X$ at EMC as a function of $z \equiv E_{J/\psi}/E_\gamma$. The singlet contributions are in the thick dotted curve, the color-octet 1S_0 contributions in the thick dashed curve (with $\langle O_8^\psi(^1S_0) \rangle = 6.6 \times 10^{-2} \text{ GeV}^3$), and the color-octet 3P_J contributions in the thin dashed curve (with $\langle O_8^\psi(^3P_J) \rangle/M_c^2 = 2.2 \times 10^{-2} \text{ GeV}^3$). The total is shown in the solid curve. The relation (1.4) allows the region between two solid curves. Here, TOT_s is the $^1S_0^{(8)}$ saturated curve and TOT_p is the $^3P_J^{(8)}$ saturated one.

Fig.7(b) The differential cross sections $d\sigma/dz$ for $\gamma + p \rightarrow J/\psi + X$ at HERA as a function of $z \equiv E_{J/\psi}/E_\gamma$. The singlet contributions are in the thick dotted curve, the color-octet 1S_0 contributions in the thick dashed curve (with $\langle O_8^\psi(^1S_0) \rangle = 6.6 \times 10^{-2} \text{ GeV}^3$), and the color-octet 3P_J contributions in the thin dashed curve (with $\langle O_8^\psi(^3P_J) \rangle/M_c^2 = 2.2 \times 10^{-2} \text{ GeV}^3$). The total is shown in the solid curve. The relation (1.4) allows the region between two solid curves. Here, TOT_s is the $^1S_0^{(8)}$ saturated curve and TOT_p is the $^3P_J^{(8)}$ saturated one.

Fig.8(a) The differential cross sections $d\sigma/dP_T^2$ for $\gamma + p \rightarrow J/\psi + X$ at HERA as a function of P_T^2 . The singlet contributions in the thick dotted curve, the color-octet 1S_0 contributions in the thick dashed curve (with $\langle O_8^\psi(^1S_0) \rangle = 6.6 \times 10^{-2} \text{ GeV}^3$), and the color-octet 3P_J contributions in the thin dashed curve (with $\langle O_8^\psi(^3P_J) \rangle/M_c^2 = 2.2 \times 10^{-2} \text{ GeV}^3$). The total is shown in the solid curve. The relation (1.4) allows the region between two solid curves. Here, TOT_s is the $^1S_0^{(8)}$ saturated curve and TOT_p is the $^3P_J^{(8)}$ saturated one.

Fig.8(b) The differential cross sections $d\sigma/dP_T^2$ for $\gamma + p \rightarrow J/\psi + X$ at HERA as a function of P_T^2 of J/ψ . The singlet contributions in the thick dotted curve, the color-octet 1S_0 contributions in the thick dashed curve (with $\langle O_8^\psi(^1S_0) \rangle = 6.6 \times 10^{-2} \text{ GeV}^3$), and the color-octet 3P_J contributions in the thin dashed curve (with $\langle O_8^\psi(^3P_J) \rangle / M_c^2 = 2.2 \times 10^{-2} \text{ GeV}^3$). The total is shown in the solid curve. The relation (1.4) allows the region between two solid curves. Here, TOT_s is the $^1S_0^{(8)}$ saturated curve and TOT_p is the $^3P_J^{(8)}$ saturated one.

Fig.9 Total inelastic J/ψ photoproduction cross section for $z < 0.8$ as a function of the square root of $s_{\gamma p}$. The singlet contributions in the thick dotted curve, the color-octet 1S_0 contributions in the thick dashed curve (with $\langle O_8^\psi(^1S_0) \rangle = 6.6 \times 10^{-2} \text{ GeV}^3$), and the color-octet 3P_J contributions in the thin dashed curve (with $\langle O_8^\psi(^3P_J) \rangle / M_c^2 = 2.2 \times 10^{-2} \text{ GeV}^3$). The total is shown in the solid curve. The relation (1.4) allows the region between two solid curves. Here, TOT_s is the $^1S_0^{(8)}$ saturated curve and TOT_p is the $^3P_J^{(8)}$ saturated one.

FIGURES

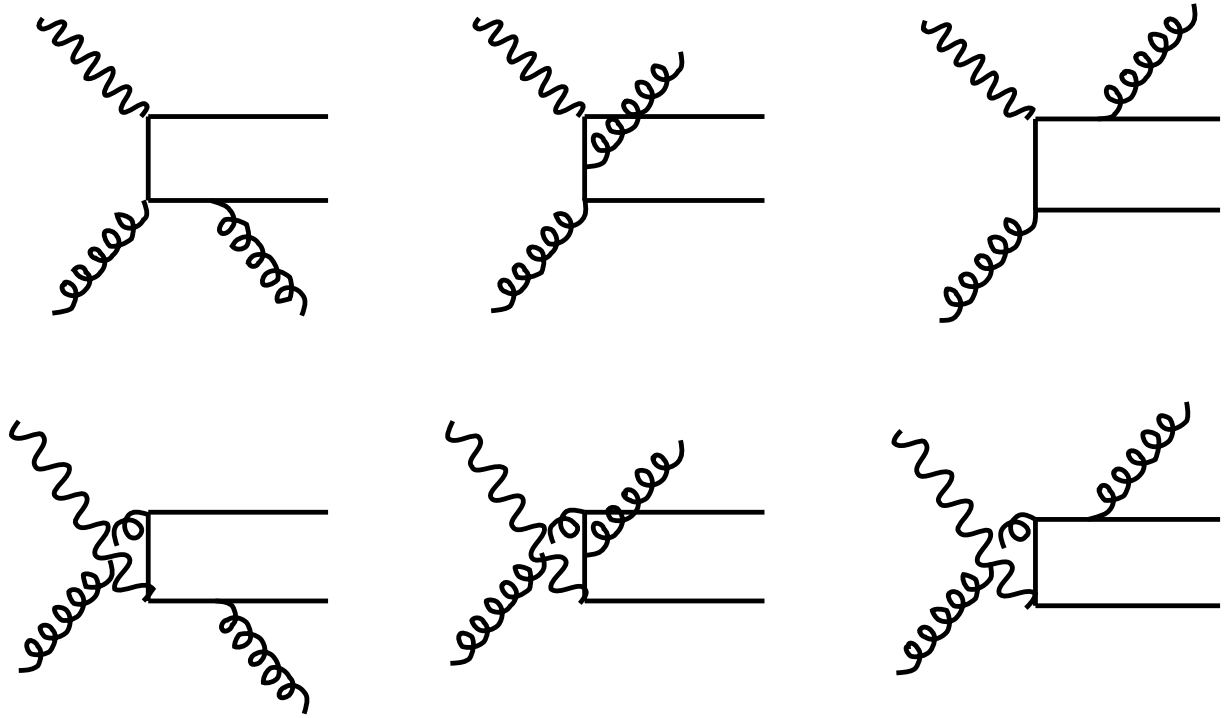


FIG. 1.

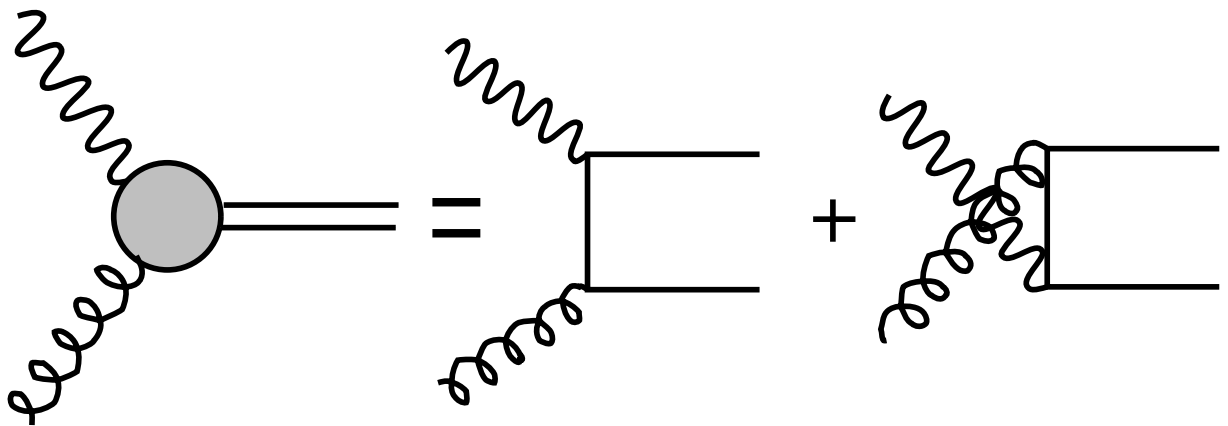


FIG. 2.

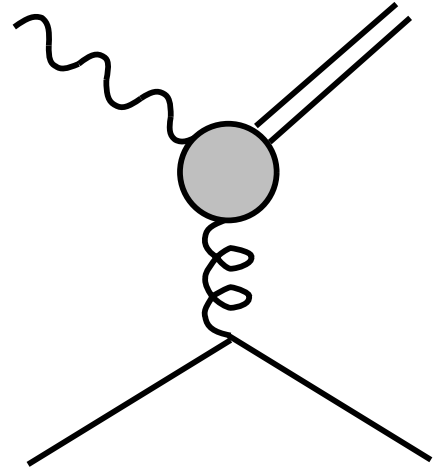
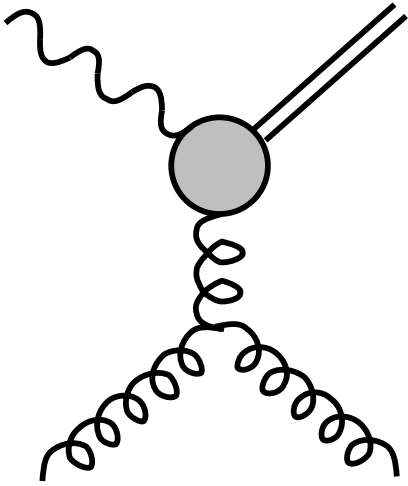


FIG. 3.

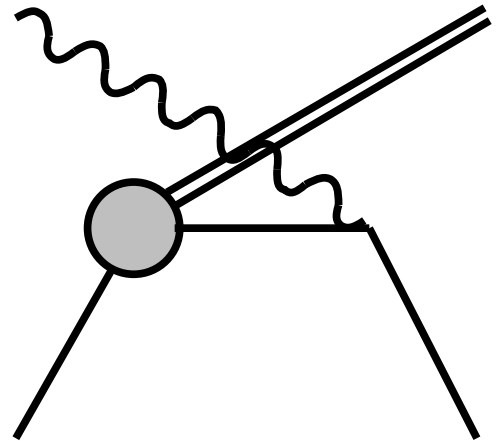
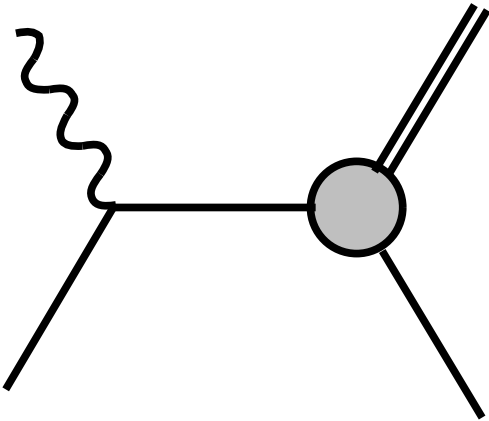


FIG. 4.

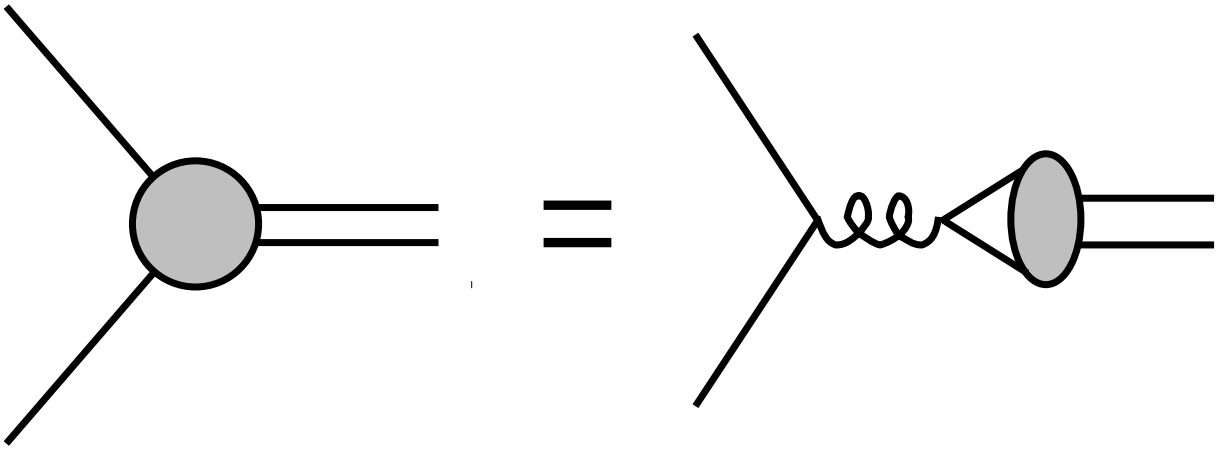


FIG. 5.

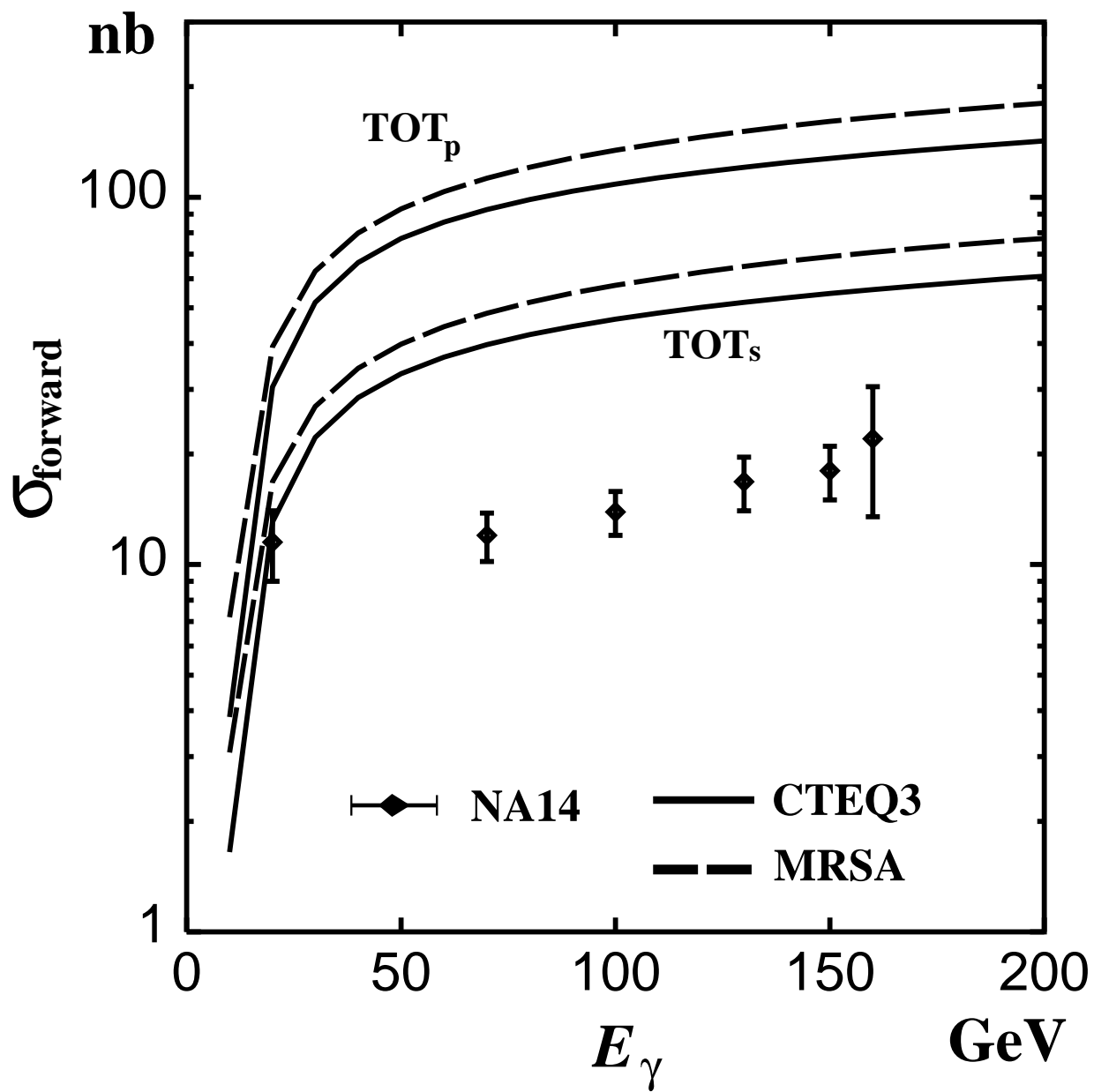


FIG. 6 (a).

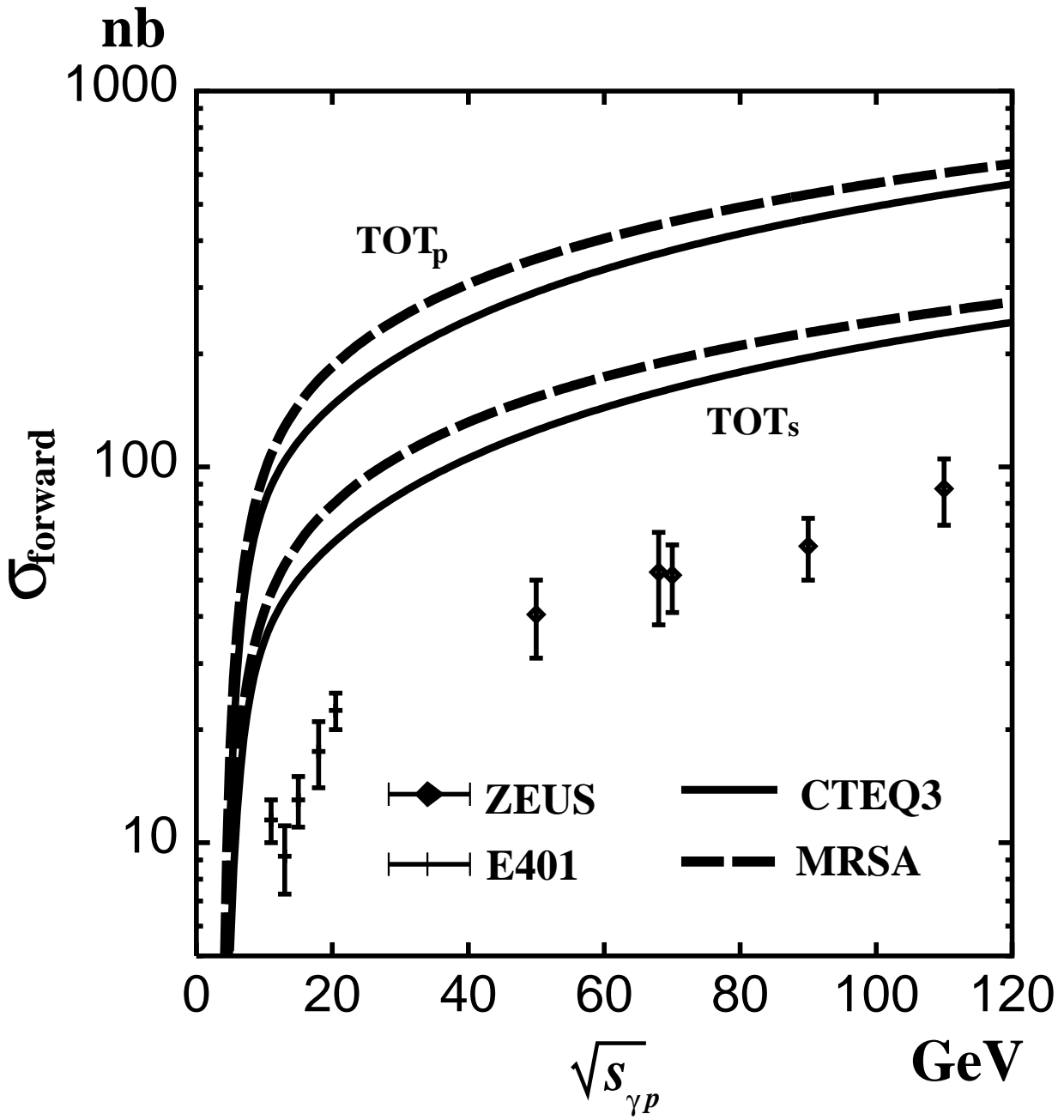


FIG. 6 (b).

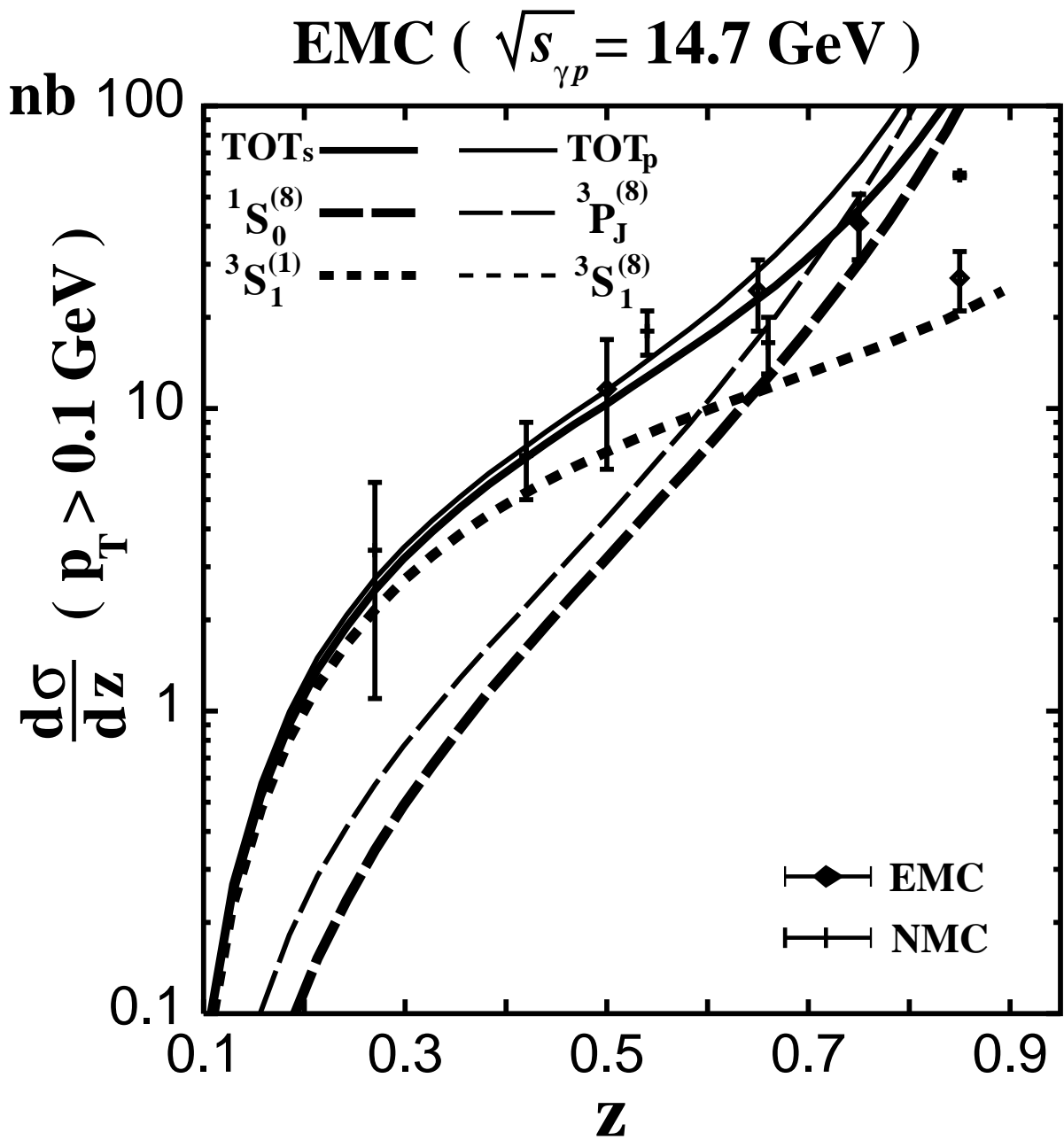


FIG. 7 (a).

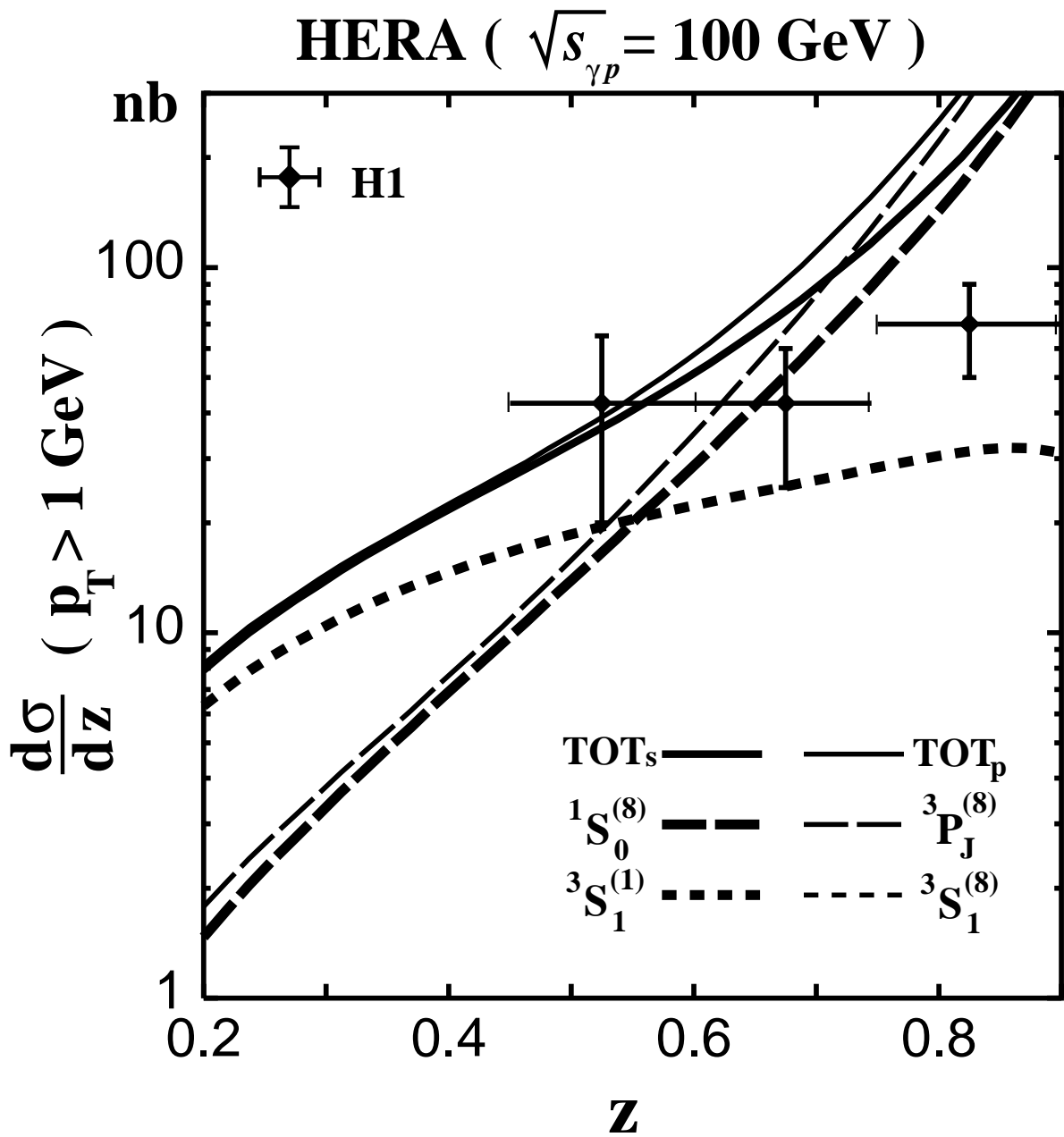


FIG. 7 (b).

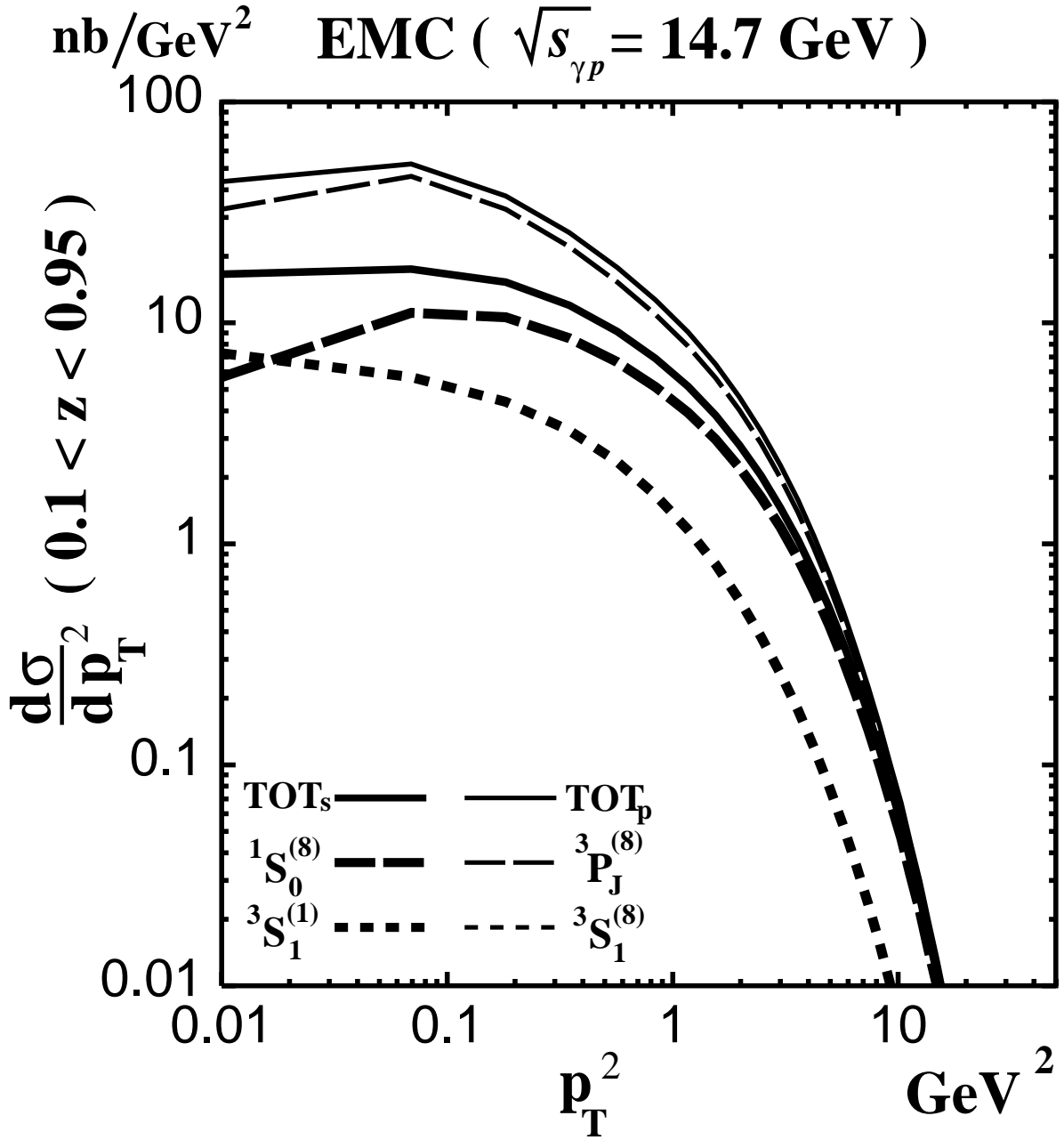


FIG. 8 (a).

nb / GeV² HERA ($\sqrt{s_{\gamma p}} = 100$ GeV)

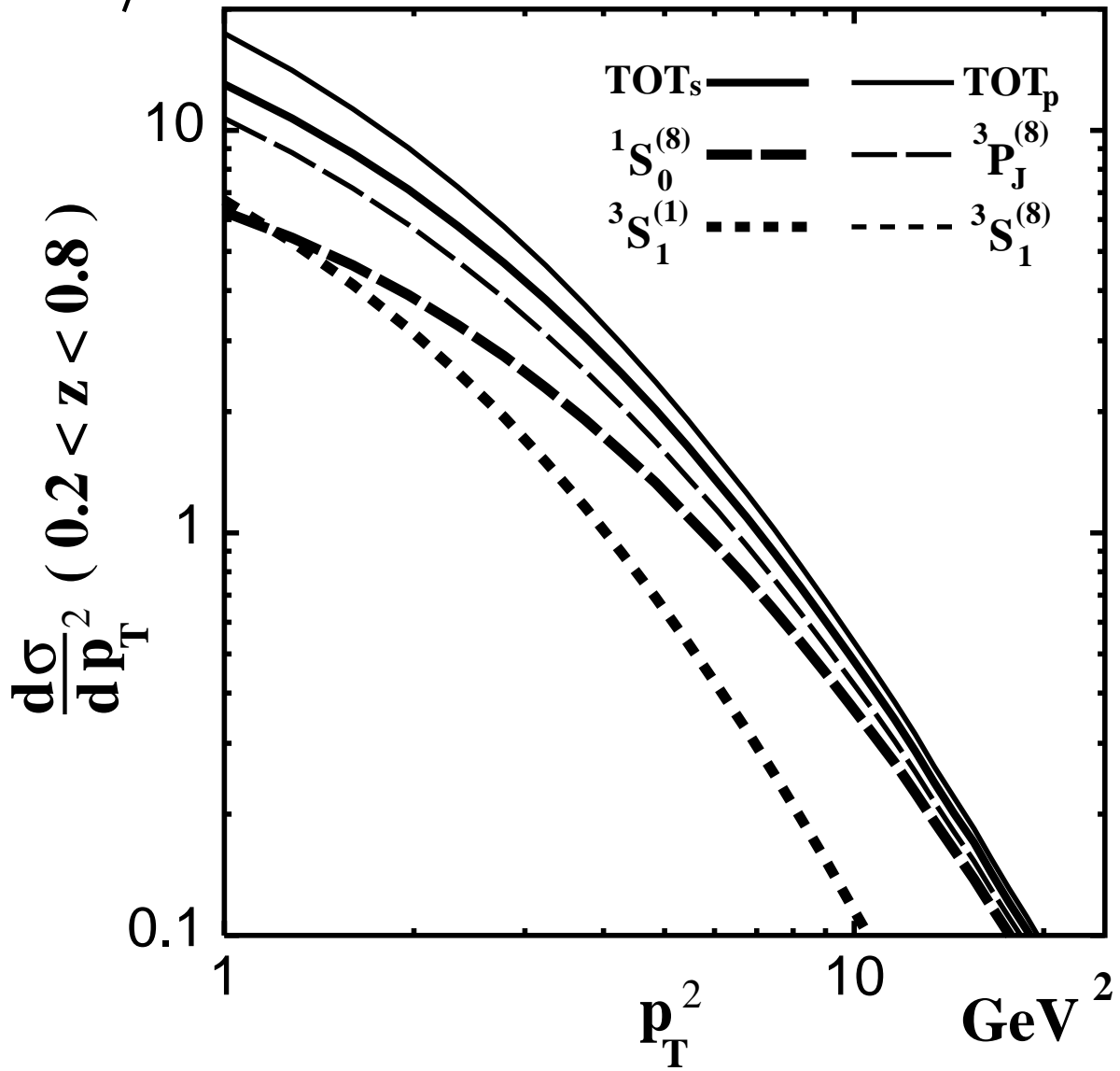


FIG. 8 (b).

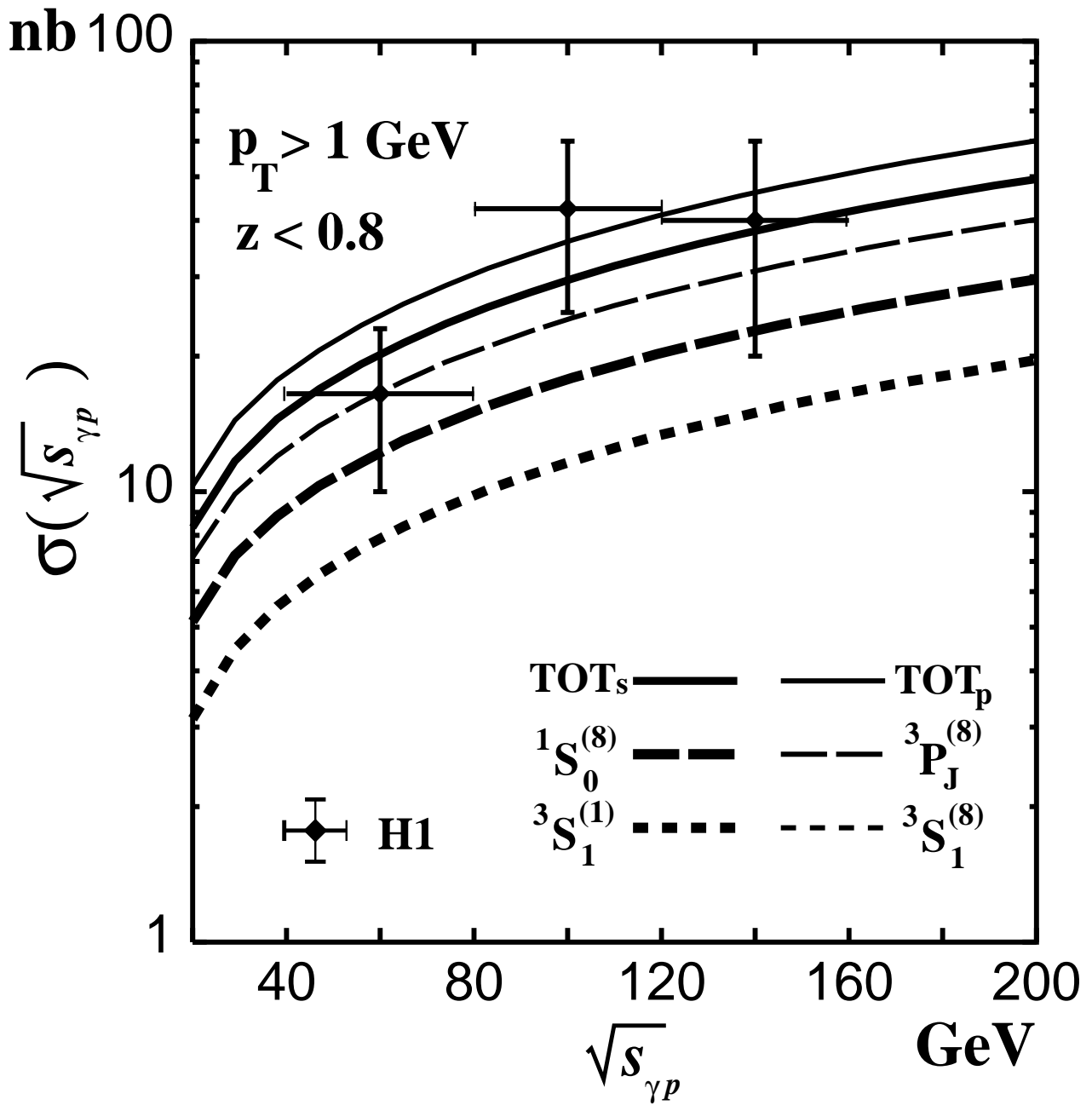


FIG. 9.